



# Search for New Physics with Precision Parity Violating Experiments

Aleksandrs Aleksejevs

Students: Cristian Griebler and Jessica Strickland  
Memorial University, Grenfell Campus, Canada

Svetlana Barkanova

Students: Matthew Bluteau and Hao Wu  
Acadia University, Canada

Yury Bystritskiy and Eduard Kuraev  
JINR, Russia

Vladimir Zykunov  
Belarusian State University of Transport, Belarus





# Outline



- Introduction
- Need for loop calculations
- One loop (NLO) calculations with different renormalization conditions
- Motivation for higher order (NNLO) contributions
  - Quadratic Contribution
  - Two-loops Contribution
- New Physics (NP) Searches using Parity-Violating Processes
  - Subtractive Scheme
  - Sensitivity of asymmetry to couplings of SM
  - NP Photon
  - NP Z
- Conclusion



# Electroweak Interactions



To calculate effects of electroweak interactions precisely we need only three input parameters:

- **Fine structure constant** arising from electromagnetic interactions.
- **W** and **Z** mass, which determine scale of weak interactions.

Parameters are chosen based on the three very precise experimental measurements:

- **Electron g-2 experiment**
- **The muon lifetime experiment**
- **Studies of the Z line shape**

Essentially all electroweak observables could be precisely calculated at the given level of radiative corrections.

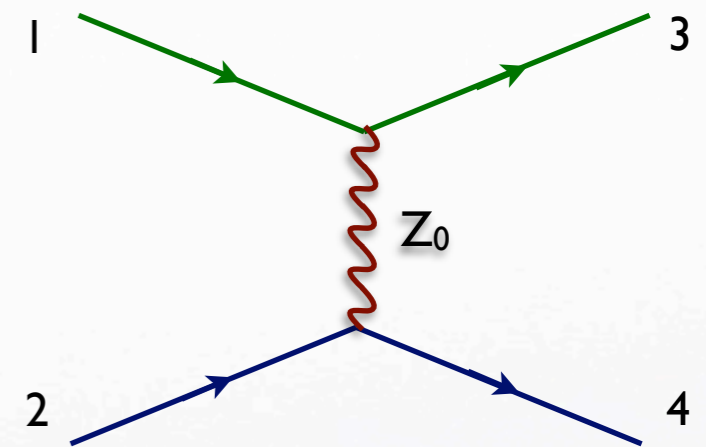
Most sensitive observables are:  $m_W$  and  $\sin^2 \theta_W = 1 - \frac{m_W^2}{m_Z^2}$



# Indirect Access to New Physics



- Many theories predict new particles, which disappeared at the time when the universe cooled.
- New physics particles are now present indirectly as interaction carriers and can be probed through precision measurements at low momentum transfer.
- To access the scale of the new physics at TeV level, it is required to push one or more experimental parameters to the extreme precision.
- Low  $Q^2$  neutral current interaction becomes sensitive to the TeV scale if:
  - $\delta(\sin^2\theta_W) \leq 0.5\%$
  - *away from the Z resonance*
- Precision Neutrino Scattering
- New Physics/Weak-Electromagnetic Interference
  - *opposite parity transitions in heavy atoms*
  - *parity-violating electron scattering*



Weak interaction provides indirect access to the new physics via interference terms between neutral weak, New Physics and QED amplitudes.

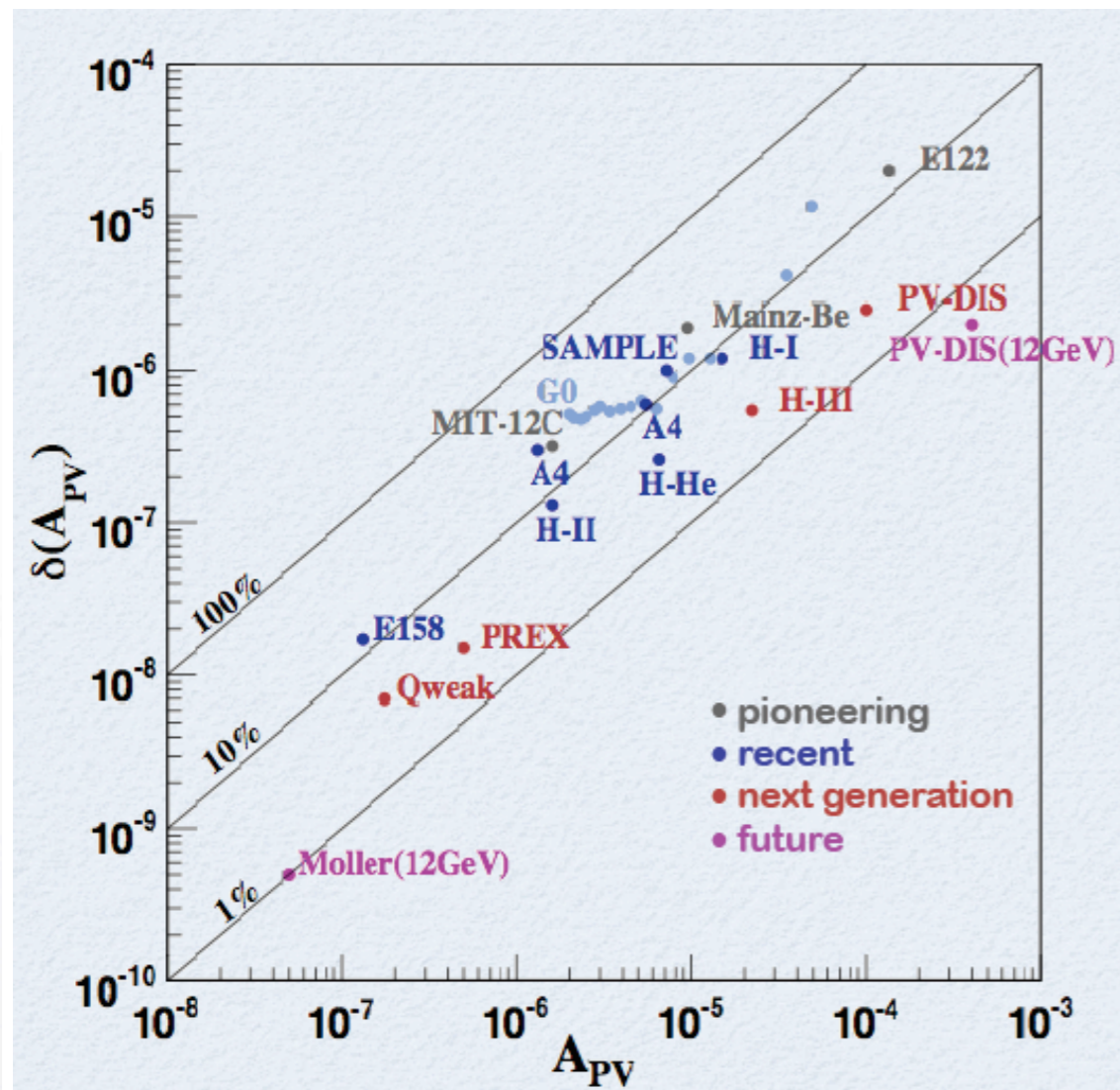


# PV Electron Scattering



Asymmetry is an observable which is directly related to the interference term:

$$A_{LR} = \frac{\sigma_L - \sigma_R}{\sigma_L + \sigma_R} \simeq \frac{2\text{Re}(M_\gamma M_Z^+ + M_\gamma M_{NP}^+ + M_Z M_{NP}^+)_{LR}}{\sigma_L + \sigma_R} \sim (10^{-5} \text{ to } 10^{-4}) \cdot Q^2$$



To access multi-TeV electron scale it is required to measure:

$$\delta(\sin^2 \theta_W) < 0.002$$

MOLLER experiment offers an unique opportunity to reach multi-TeV scale and will become complimentary to the LHC direct searches of the New Physics

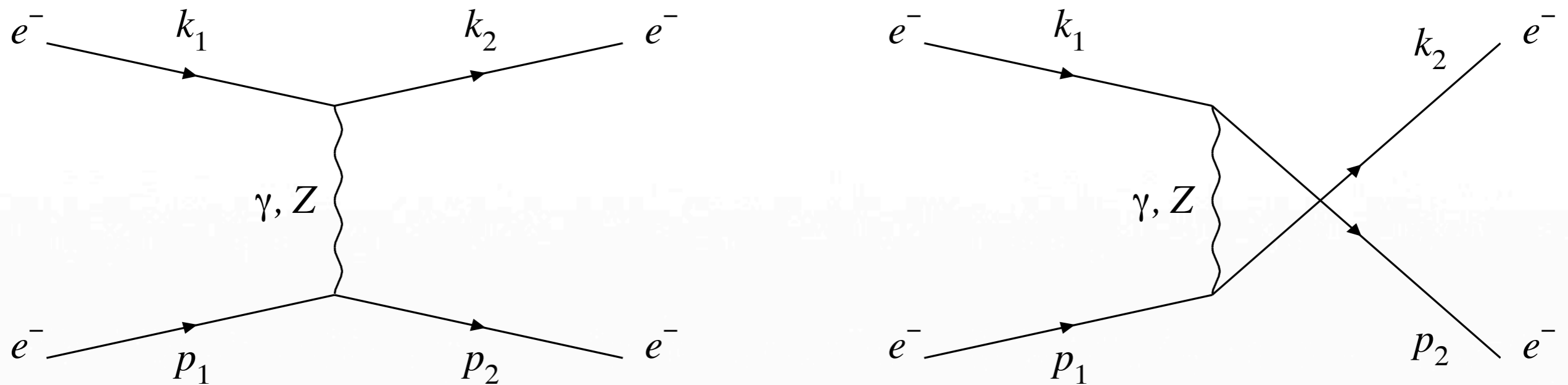


# Møller scattering at the tree level



The process of electron–electron scattering (Møller process)

C. Møller, *Annalen der Physik* 406, 531 (1932)



Straightforward and clean process!

$$A_{LR} = \frac{\sigma_{LL} + \sigma_{LR} - \sigma_{RL} - \sigma_{RR}}{\sigma_{LL} + \sigma_{LR} + \sigma_{RL} + \sigma_{RR}} = \frac{\sigma_{LL} - \sigma_{RR}}{\sigma_{LL} + 2\sigma_{LR} + \sigma_{RR}}$$

$$A_{LR}^0 = \frac{s}{2m_W^2} \frac{y(1-y)}{1+y^4+(1-y)^4} \frac{1-4s_W^2}{s_W^2}, \quad y = -t/s$$

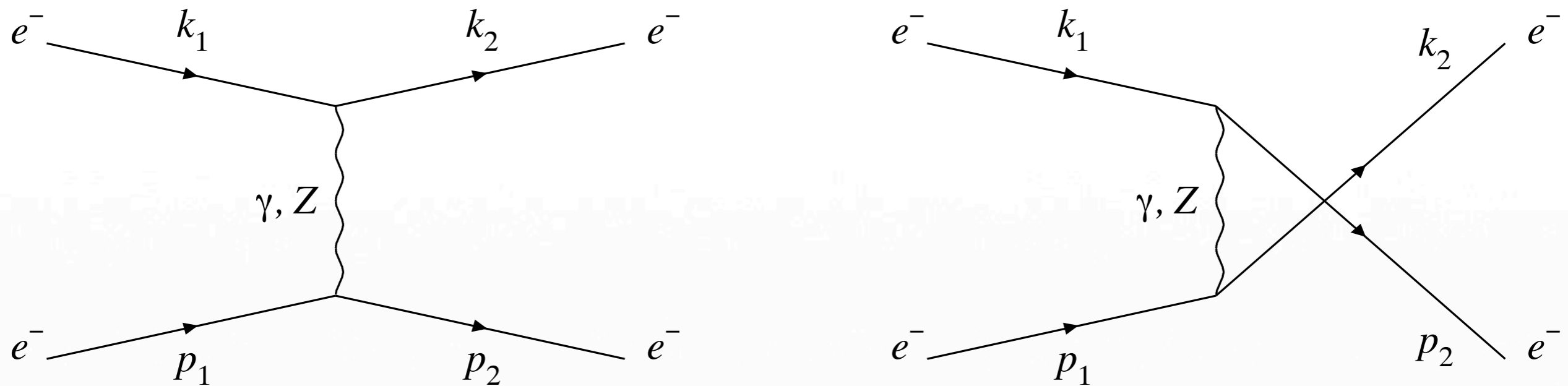


# Møller scattering at the tree level



The process of electron–electron scattering (Møller process)

C. Møller, *Annalen der Physik* 406, 531 (1932)



Straightforward and clean process!

$$A_{LR} = \frac{\sigma_{LL} + \sigma_{LR} - \sigma_{RL} - \sigma_{RR}}{\sigma_{LL} + \sigma_{LR} + \sigma_{RL} + \sigma_{RR}} = \frac{\sigma_{LL} - \sigma_{RR}}{\sigma_{LL} + 2\sigma_{LR} + \sigma_{RR}}$$

$$A_{LR}^0 = \frac{s}{2m_W^2} \frac{y(1-y)}{1+y^4+(1-y)^4} \frac{1-4s_W^2}{s_W^2}, \quad y = -t/s$$



# Motivation



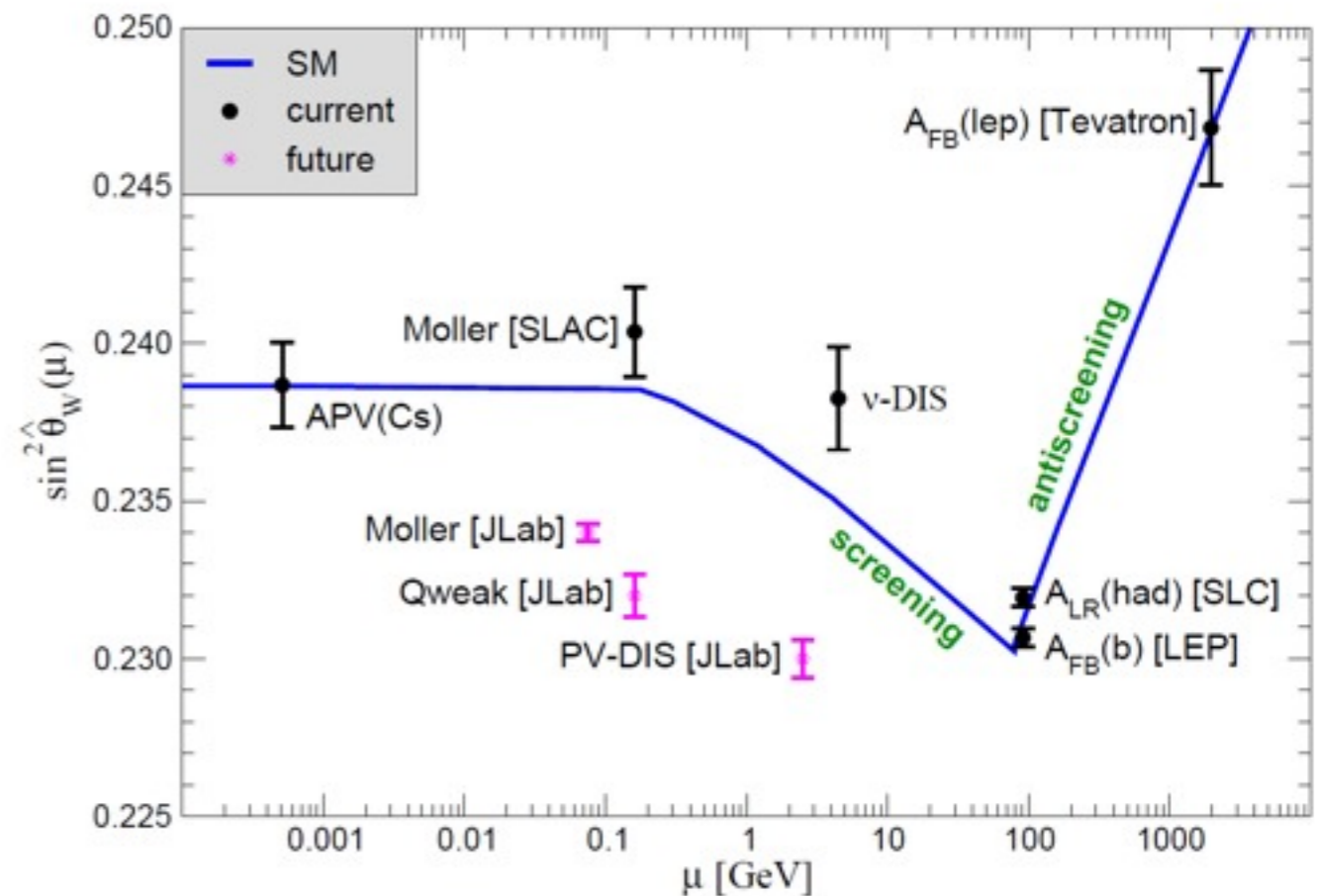
The first observation of Parity Violation in Møller scattering was made by E-158 experiment at SLAC:

$$Q^2 = 0.026 \text{ GeV}^2, A_{LR} = (1.31 \pm 0.14(\text{stat.}) \pm 0.10(\text{syst.})) \times 10^{-7}$$

$$\sin^2(\hat{\theta}_W) = 0.2403 \pm 0.0013 \text{ in } \overline{MS}$$

MOLLER, planned at JLab following the 11 GeV upgrade, will offer a new level of sensitivity and measure the parity-violating asymmetry in the scattering of longitudinally polarized electrons off unpolarized target to a precision of 0.73 ppb.

That would allow a determination of the weak mixing angle with an uncertainty of about 0.1%, a factor of five improvement in fractional precision over the measurement by E-158.



J. Benesch et al., MOLLER Proposal to PAC34, 2008





# Motivation



Although PV asymmetry ( $A_{LR} \sim 10^{-8}$ ) is very small, the accuracy of modern experiments exceeds the accuracy of the theoretical result in Born approximation. One-loop contribution was found to be rather big in the previous works:

[A. Czarnecki, W. J. Marciano, Phys. Rev. D53, 1066 \(1996\);](#)

[A. Denner, S. Pozzorini, Eur. Phys. J. C7, 185 \(1999\);](#)

[A. Aleksejevs, S. Barkanova, A. Ilyichev, V. Zykunov, Phys. Rev. D82, 093013 \(2010\).](#)

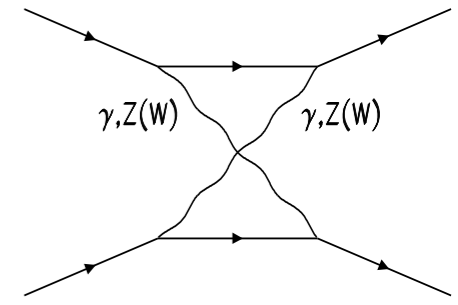
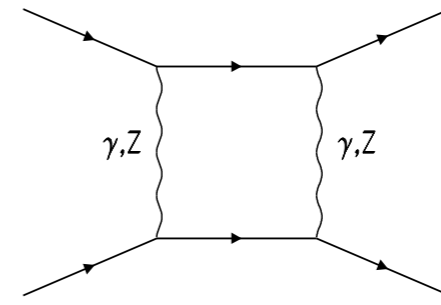
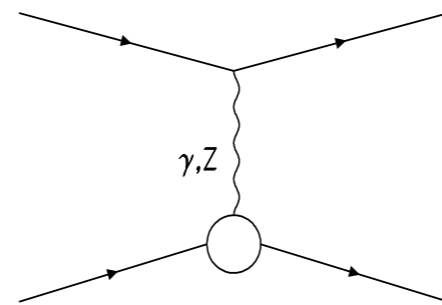
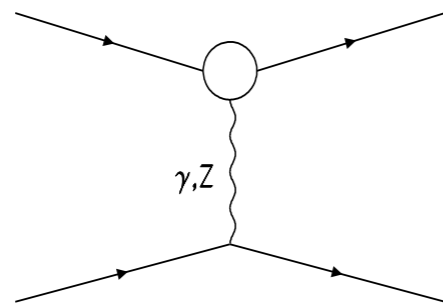
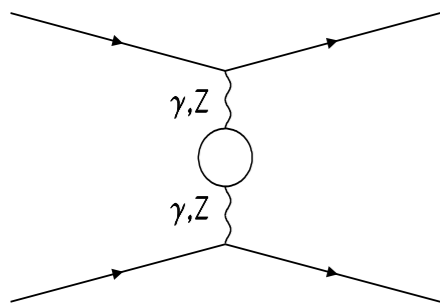
- Theoretical approach to control precision:
  - Make sure that everything is correct for the given level of perturbation (start with one loop)
    - For that we choose and compare two approaches: “by hand” and computer based using on-shell renormalization and using two different renormalization conditions (RC).
  - Determine if higher order effects (two-loops) are important
    - For that we compare results in two renormalization schemes (RS): on-shell and constrained differential renormalization (CDR). Size of the difference between RS will point out importance of higher order effects:  
[W. Hollik and H.-J. Timme, Z. Phys. C. 33, 125 \(1986\).](#)



# One Loop



# One-loop



$$\sigma = \frac{\pi^3}{2s} |M_0 + M_1|^2 = \frac{\pi^3}{2s} \left( \underbrace{M_0 M_0^+}_{\propto \alpha^2} + \underbrace{2\text{Re}M_1 M_0^+}_{\propto \alpha^3} + \underbrace{M_1 M_1^+}_{\propto \alpha^4} \right) = \sigma_0 + \sigma_1 + \sigma_Q$$

$$\sigma_1 = \sigma_1^{BSE} + \sigma_1^{Ver} + \sigma_1^{Box}$$

- Calculated in on-shell renormalization using:
  - Computer based using Feynarts, FormCalc, LoopTools and Form
    - T. Hahn, [Comput. Phys. Commun. 140 418 \(2001\)](#);
    - T. Hahn, M. Perez-Victoria, [Comput. Phys. Commun. 118, 153 \(1999\)](#);
    - J. Vermaseren, (2000) [[arXiv:math-ph/0010025](#)]

• “By hand” using approximations in small energy region  $\frac{\{t, u\}}{m_{Z,W}^2} \ll 1$ , for  $\sqrt{s} \ll 30 \text{ GeV}$  and high energy approximation for  $\sqrt{s} \gg 500 \text{ GeV}$

- For a gauge invariant set, physical results should be invariant under different fields renormalization conditions.
- Renormalization constants are fixed by the renormalization conditions.
- Consider two classes:
  1. The first determines the renormalization of the parameters and is related to physical observables at a given order of perturbation theory. These conditions are identical in both Hollik RC (HRC) and Denner RC (DRC).

$$\text{Re}\hat{\Sigma}_T^W(m_W^2) = \text{Re}\hat{\Sigma}_T^Z(m_Z^2) = \text{Re}\hat{\Sigma}^f(m_f^2) = 0,$$

$$\hat{\Gamma}_\mu^{ee\gamma}(k^2 = 0, p^2 = m^2) = ie\gamma_\mu.$$

2. The second class fixes the renormalization of fields and is related to the Green's functions and has no effect on calculations of S-matrix elements.

$$\hat{\Sigma}_T^{\gamma Z}(0) = 0, \quad \frac{\partial}{\partial k^2} \hat{\Sigma}_T^\gamma(0) = 0$$

$$\hat{\Sigma}_T^{\gamma Z}(0) = 0, \quad \frac{\partial}{\partial k^2} \hat{\Sigma}_T^\gamma(0) = 0$$

$$\text{Re}\hat{\Sigma}_T^{\gamma Z}(m_Z^2) = 0, \quad \text{Re}\frac{\partial}{\partial k^2} \hat{\Sigma}_T^Z(m_Z^2) = 0, \quad \text{Re}\frac{\partial}{\partial k^2} \hat{\Sigma}_T^W(m_W^2) = 0.$$



# One-loop: renormalization conditions



## Hollik RC (“by hand”)

$$\begin{aligned} \delta Z_\gamma^{(H)} &= -\frac{\partial}{\partial k^2} \Sigma_T^\gamma(0), \\ \delta Z_Z^{(H)} &= \frac{\partial}{\partial k^2} \Sigma_T^\gamma(0) - 2 \frac{c_W^2 - s_W^2}{s_W c_W} \frac{\Sigma_T^{\gamma Z}(0)}{m_Z^2} \\ &\quad + 2 \frac{c_W^2 - s_W^2}{s_W^2} \left( \frac{\delta m_Z^2}{m_Z^2} - \frac{\delta m_W^2}{m_W^2} \right), \\ \delta Z_W^{(H)} &= \frac{\partial}{\partial k^2} \Sigma_T^\gamma(0) - 2 \frac{c_W}{s_W} \frac{\Sigma_T^{\gamma Z}(0)}{m_Z^2} \\ &\quad + \frac{c_W^2}{s_W^2} \left( \frac{\delta m_Z^2}{m_Z^2} - \frac{\delta m_W^2}{m_W^2} \right), \\ \delta Z_{Z\gamma}^{(H)} &= \frac{c_W s_W}{c_W^2 - s_W^2} \left( \delta Z_Z^{(H)} - \delta Z_\gamma^{(H)} \right). \end{aligned}$$

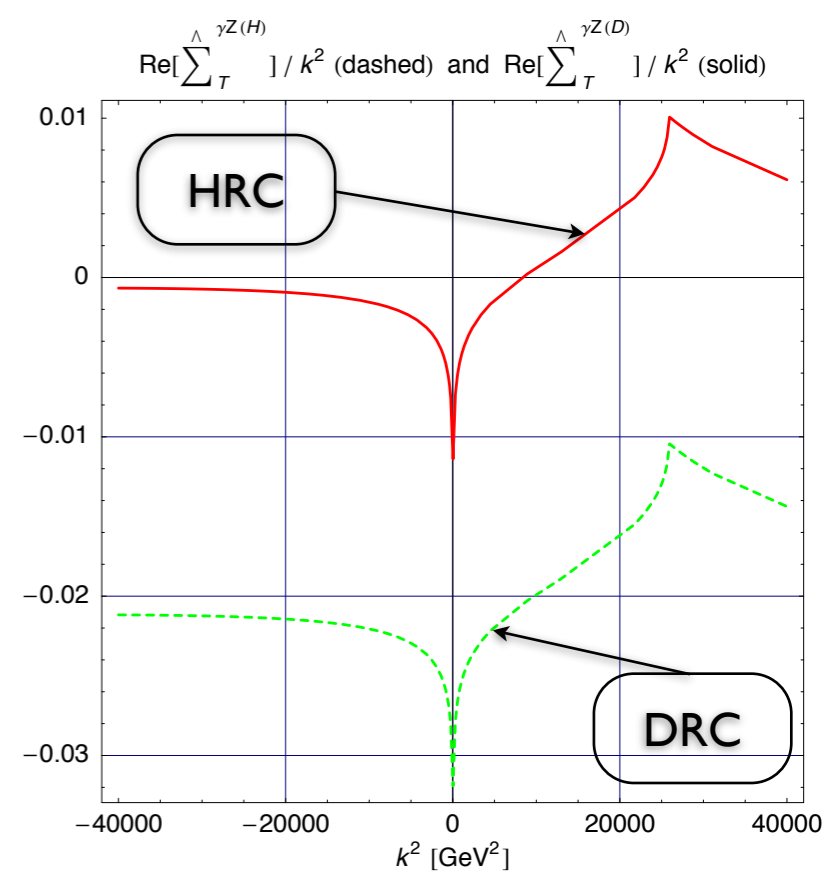
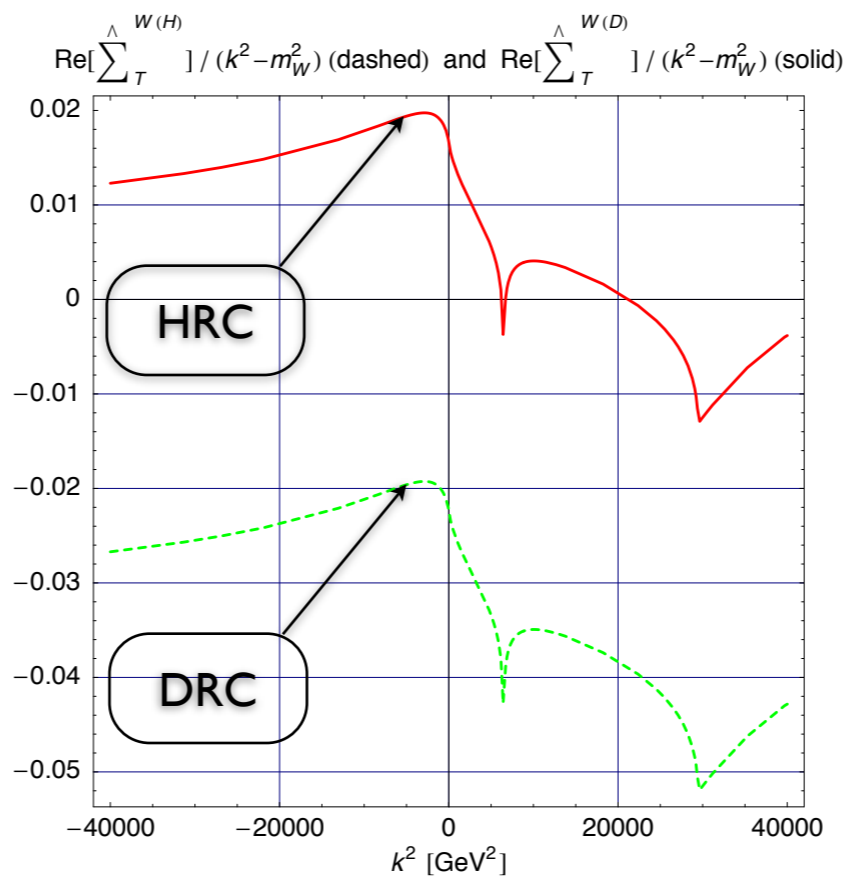
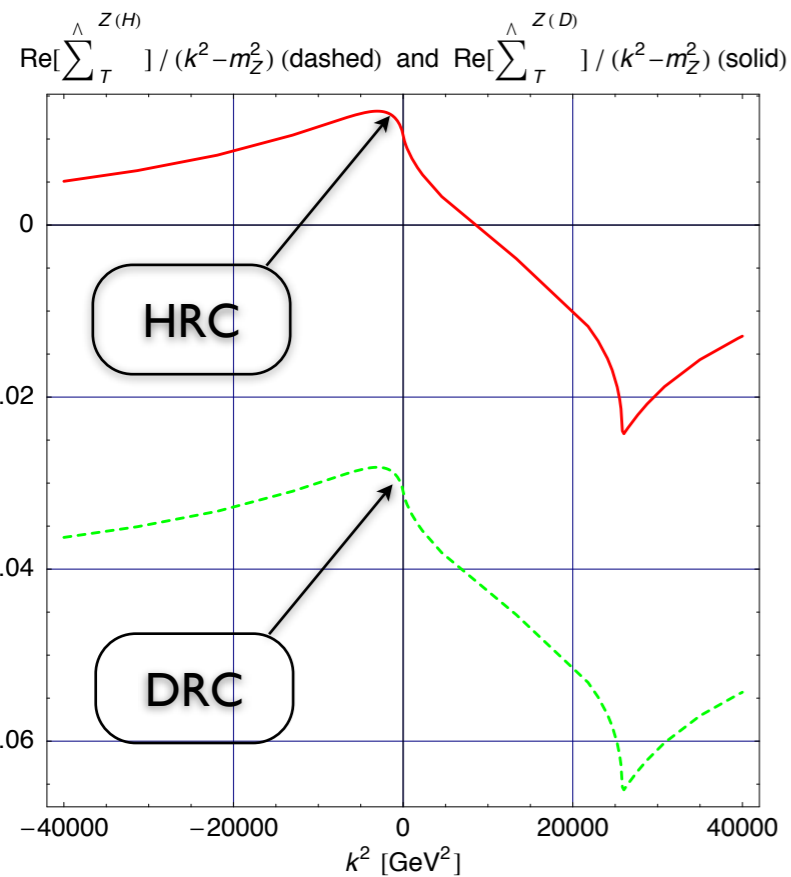
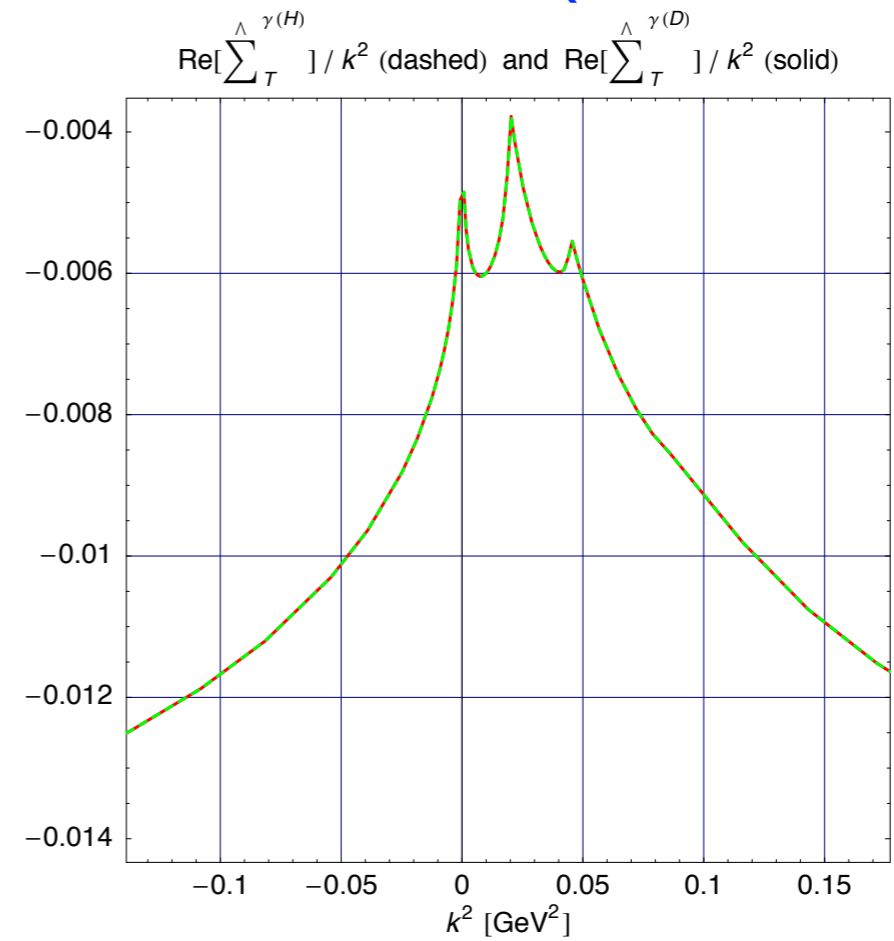
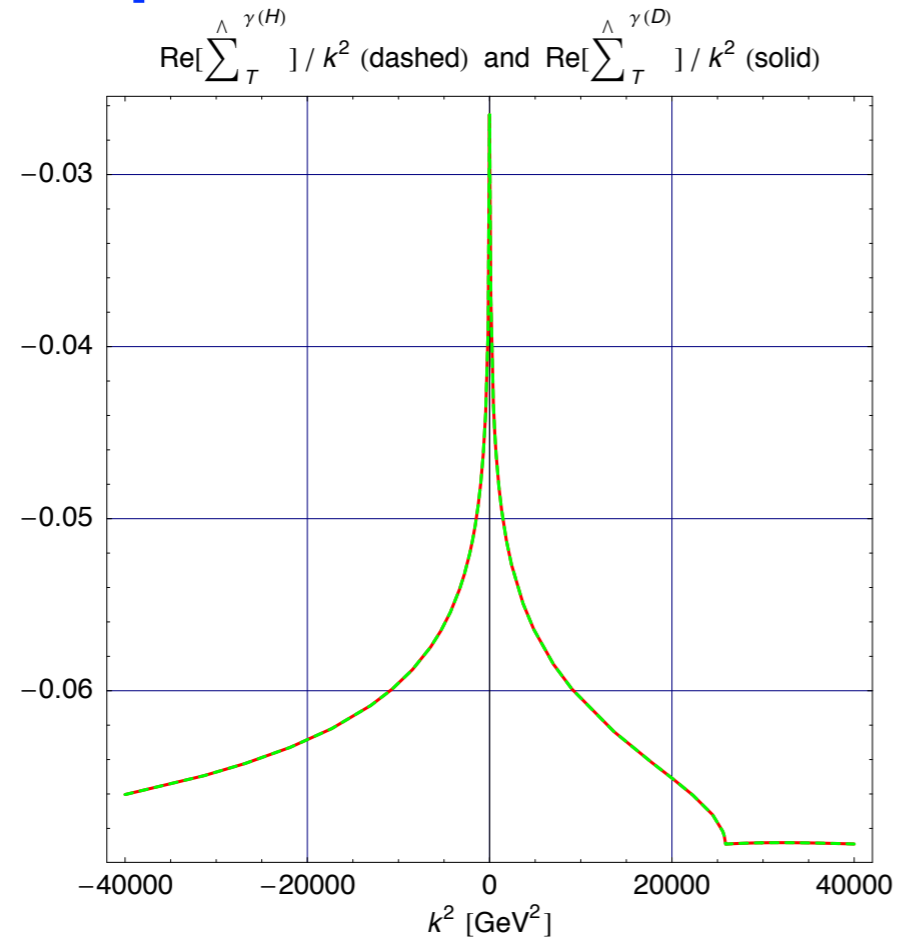
## Denner RC (computer based)

$$\begin{aligned} \delta Z_W^{(D)} &= -\text{Re} \frac{\partial}{\partial k^2} \Sigma_T^W(m_W^2), \\ \delta Z_Z^{(D)} &= -\text{Re} \frac{\partial}{\partial k^2} \Sigma_T^Z(m_Z^2), \\ \delta Z_{Z\gamma}^{(D)} &= \frac{2}{m_Z^2} \text{Re} \Sigma_T^{\gamma Z}(0), \quad \delta Z_{\gamma Z}^{(D)} = -\frac{2}{m_Z^2} \text{Re} \Sigma_T^{\gamma Z}(m_Z^2), \\ \delta Z_\gamma^{(D)} &= -\frac{\partial}{\partial k^2} \Sigma_T^\gamma(0). \end{aligned}$$

W. Hollik, Fortschr. Phys. 38, 165 (1990).

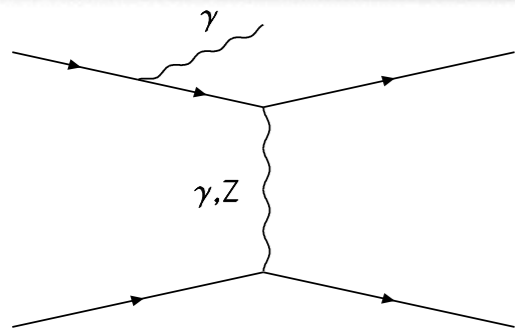
A. Denner, Fortschr. Phys. 41, 307 (1993).

# One-loop: renormalization conditions (Self Energies)

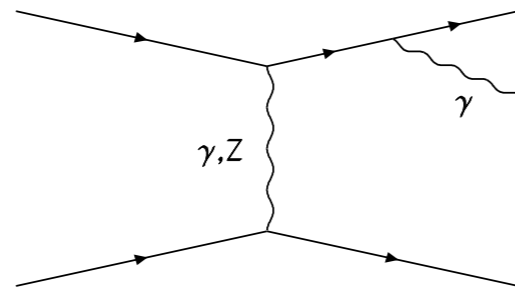




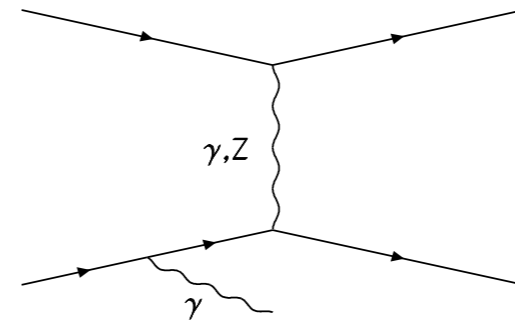
# One-loop: photon emission



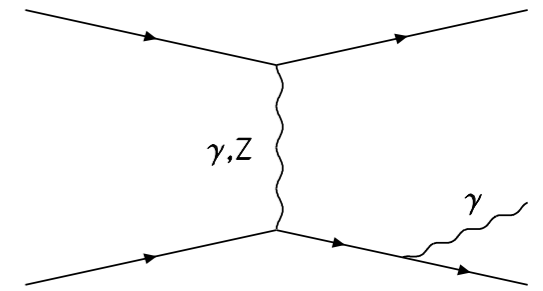
(1)



(2)



(3)



(4)

$$\sigma_{IR}^{Ver} + \sigma_{IR}^{\gamma\gamma-box} + \sigma_{IR}^{\gamma Z} = -\frac{2\alpha}{\pi} \log \frac{s}{\lambda^2} \log \frac{tu}{em^2 s} \sigma_0$$

$$\sigma^R = \underbrace{\sigma_{IR}^R}_{\text{red}} + \underbrace{\sigma_H^R}_{\text{blue}}$$

$$\underbrace{\sigma_{IR}^R}_{\text{red}} = \frac{2\alpha}{\pi} \left( \log \frac{4\omega^2}{\lambda^2} \log \frac{tu}{em^2 s} - \frac{1}{2} \log^2 \frac{s}{em^2} + \frac{1}{2} - \frac{\pi^2}{6} + \frac{1}{2} \log^2 \frac{u}{t} \right) \sigma_0$$

$$\underbrace{\sigma_H^R}_{\text{blue}} = \frac{2\alpha}{\pi} \log \frac{\Omega^2}{\omega^2} \log \frac{tu}{em^2 s} \sigma_0 + \sigma_H^{R,\Omega}$$



# One-loop: results



The relative correction to the Born asymmetry  $A^0_{LR}$  is defined as follows:

$$\delta_A^C = \frac{A_{LR}^C - A_{LR}^0}{A_{LR}^0}$$

where index C means a specific contribution (C = BSE, Ver, Box, ... ),  $A^0_{LR}$  is the Born asymmetry, and  $A^C_{LR}$  is the total asymmetry including electroweak radiative corrections.

Input parameters:  $\alpha=1/137.035999$ ,  
 $m_W = 80.398$  GeV,  
 $m_Z = 91.1876$  GeV.

$\sqrt{s}$ , GeV	Result of Denner and Pozzorini	Our result
100	-0.2787	-0.2790
500	-0.3407	-0.3406
2000	-0.9056	-0.9066

Comparison of our result for the weak correction to asymmetry with the result of [arXiv:hep-ph/9807446](https://arxiv.org/abs/hep-ph/9807446).





# One-loop: results

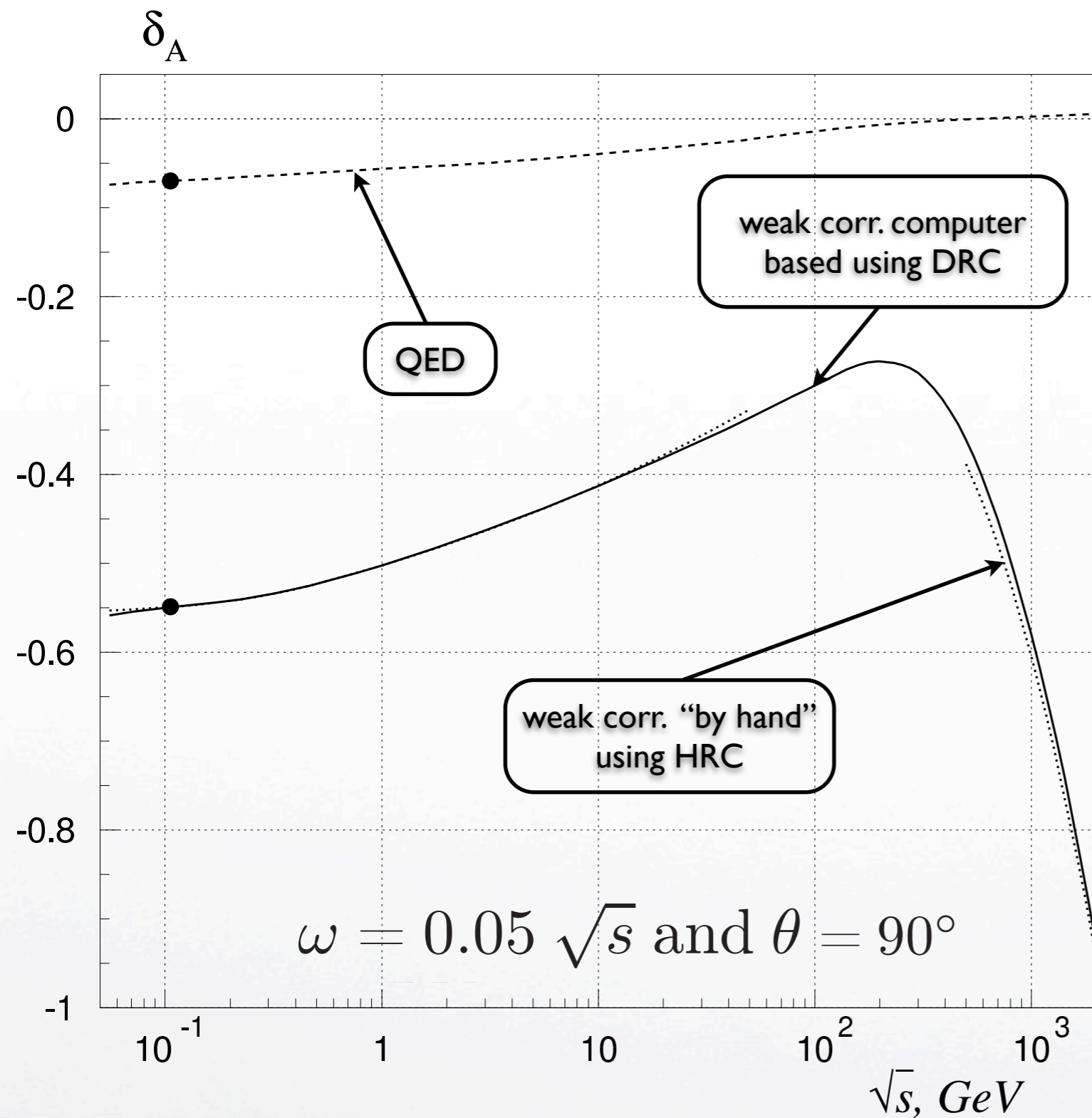


The Born asymmetry  $A_{LR}^0$  and the structure of relative *weak* corrections to it for  $E_{\text{lab}} = 11$  GeV at different  $\theta$ .

$\theta, ^\circ$	20	30	40	50	60	70	80	90
$A_{LR}^0$ , ppb	6.63	15.19	27.45	43.05	60.69	77.68	90.28	94.97
$\gamma\gamma$ -SE, DRC	-0.0043	-0.0049	-0.0054	-0.0058	-0.0062	-0.0064	-0.0066	-0.0067
$\gamma\gamma$ -SE, HRC	-0.0043	-0.0049	-0.0054	-0.0058	-0.0062	-0.0064	-0.0066	-0.0067
$\gamma Z$ -SE, DRC	-0.2919	-0.2916	-0.2914	-0.2912	-0.2911	-0.2910	-0.2909	-0.2909
$\gamma Z$ -SE, HRC	-0.6051	-0.6043	-0.6042	-0.6038	-0.6034	-0.6031	-0.6028	-0.6028
$ZZ$ -SE, DRC	-0.0105	-0.0105	-0.0105	-0.0105	-0.0105	-0.0105	-0.0105	-0.0105
$ZZ$ -SE, HRC	0.0309	0.0309	0.0309	0.0309	0.0309	0.0309	0.0309	0.0309
HV, DRC	-0.2946	-0.2633	-0.2727	-0.2703	-0.2714	-0.2712	-0.2711	-0.2710
HV, HRC	-0.0015	-0.0012	-0.0010	-0.0009	-0.0008	-0.0007	-0.0007	-0.0007
$ZZ$ -box, exact	-0.0013	-0.0013	-0.0013	-0.0013	-0.0013	-0.0013	-0.0013	-0.0013
$ZZ$ -box, approx.	-0.0013	-0.0013	-0.0013	-0.0013	-0.0013	-0.0013	-0.0013	-0.0013
$WW$ -box, exact	0.0239	0.0238	0.0238	0.0239	0.0239	0.0238	0.0238	0.0238
$WW$ -box, approx.	0.0238	0.0238	0.0238	0.0238	0.0238	0.0238	0.0238	0.0238
total <i>weak</i> , DRC, exact	-0.5643	-0.5430	-0.5508	-0.5489	-0.5500	-0.5495	-0.5493	-0.5493
total <i>weak</i> , HRC, approx.	-0.5526	-0.5514	-0.5511	-0.5505	-0.5500	-0.5496	-0.5493	-0.5493



# One-loop: results and comparison



The relative weak (solid line in DRC (semi-automated) and dotted line in HRC ("by hand") and QED (dashed line) corrections to the Born asymmetry  $A_{LR}^0$  versus  $\sqrt{s}$  at  $\theta = 90^\circ$ .

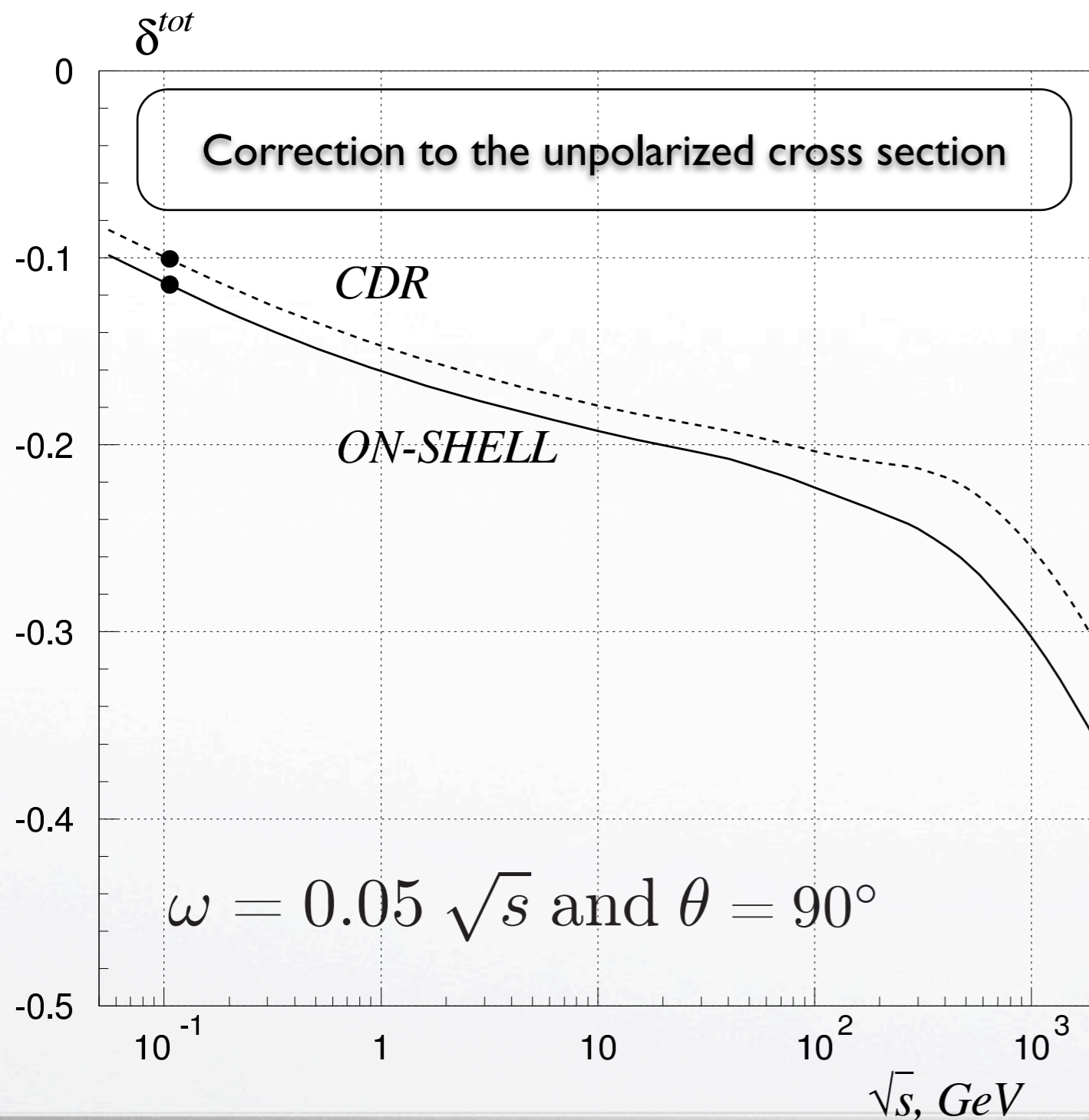
The filled circle corresponds to our predictions for the MOLLER experiment.



# Motivation for Higher Order Corrections

# One-loop in different schemes: cross section

- Constrained Differential Renormalization (CDR): [F. del Aguila et al., Phys. Lett. B 419 263 \(1998\)](#)



$$\delta^{tot} = (\sigma^{tot} - \sigma^0) / \sigma^0$$

In the region of small energies, the difference between the two schemes is almost constant and rather small ( $\sim 0.01$ ), but grows at  $\sqrt{s} \geq m_Z$ .

At small energies, the correction to the cross section is dominated by the QED contribution. However, in the high-energy region the weak correction becomes comparable to QED. Since the difference between the on-shell and CDR results grows substantially as the weak correction becomes larger, it is clear that for an observable such as the PV asymmetry the difference between the on-shell and CDR schemes will be sizable for the entire spectrum of energies  $\sqrt{s} < 2000$  GeV.



# Higher Order Corrections



# Higher order corrections

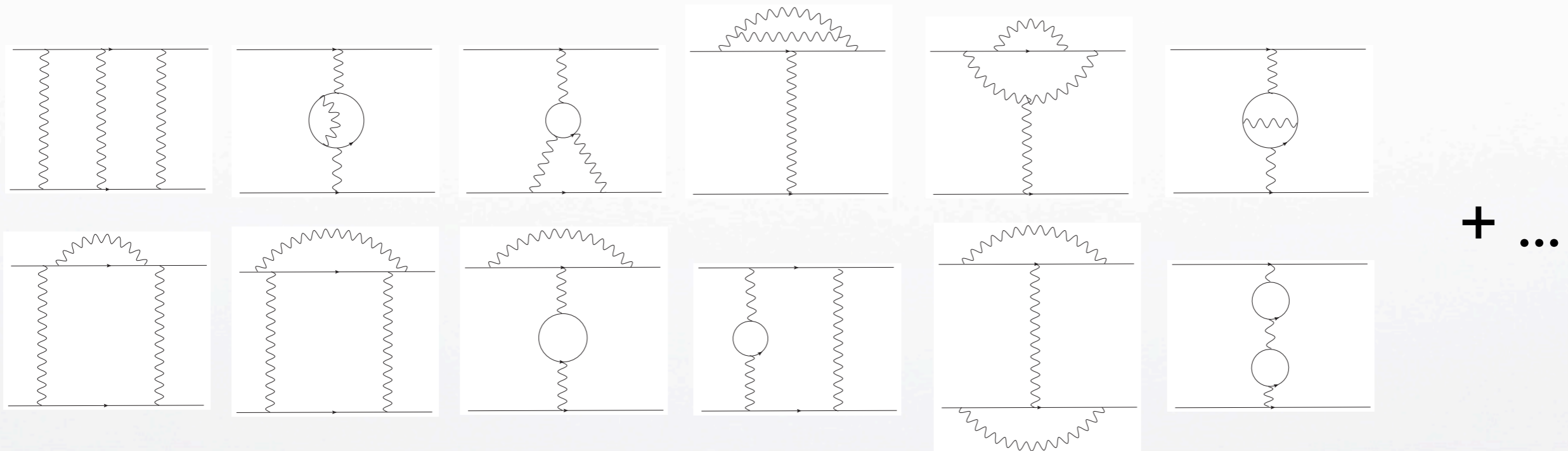


The Next-to-Next-to-Leading Order (NNLO) EWC to the Born ( $\sim M_0 M_0^+$ ) cross section can be divided into two classes:

- Q-part induced by quadratic one-loop amplitudes  $\sim M_1 M_1^+$ , and
- T-part – the interference of Born and two-loop diagrams  $\sim 2\text{Re}M_0 M_{2\text{-loop}}^+$ .

$$\sigma = \frac{\pi^3}{2s} |M_0 + M_1|^2 = \frac{\pi^3}{2s} \left( \underbrace{M_0 M_0^+}_{\propto \alpha^2} + \underbrace{2\text{Re}M_1 M_0^+}_{\propto \alpha^3} + \underbrace{M_1 M_1^+}_{\propto \alpha^4} \right) = \sigma_0 + \sigma_1 + \sigma_Q$$

$$\sigma_T = \frac{\pi^3}{s} \text{Re}M_2 M_0^+ \propto \alpha^4$$





# Quadratic Contribution



# Quadratic correction: IR part



Differential quadratic cross section  $\sigma_Q$  written as sums of  $\lambda$ -dependent (IRD-terms) and  $\lambda$ -independent (infrared-finite) parts.

$$\sigma_Q = \frac{\pi^3}{2s} M_1 M_1^+ = \underbrace{\sigma_Q^\lambda}_{\text{IRD-terms}} + \underbrace{\sigma_Q^f}_{\text{infrared-finite}}$$

$$\frac{\pi^3}{2s} M_1^{\lambda+} (M_1^\lambda + 2M_1^f) = \frac{1}{4} \left(\frac{\alpha}{\pi}\right)^2 \text{Re} \left[ \delta_1^{\lambda*} (\delta_1^\lambda + 2\delta_1^f) \right] \sigma_0 \quad \left(\frac{\alpha}{\pi}\right)^2 \delta_Q^f \sigma_0$$

$$\delta_1^\lambda = 4B \log \frac{\lambda}{\sqrt{s}}$$

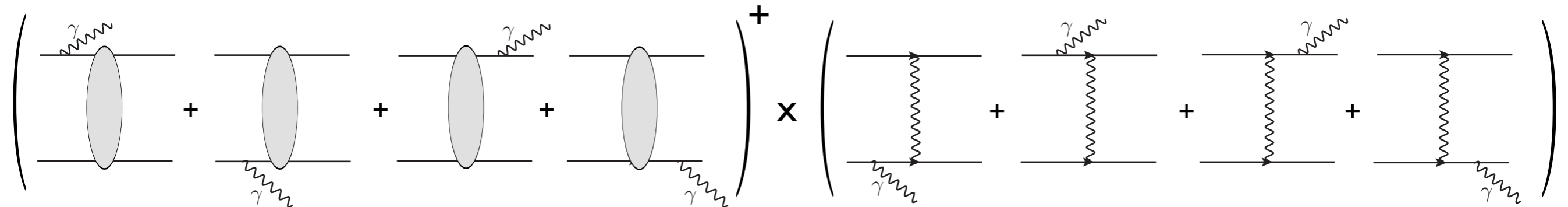
$$B = \log \frac{tu}{m^2 s} - 1 + i\pi$$



# Quadratic correction: photon emission

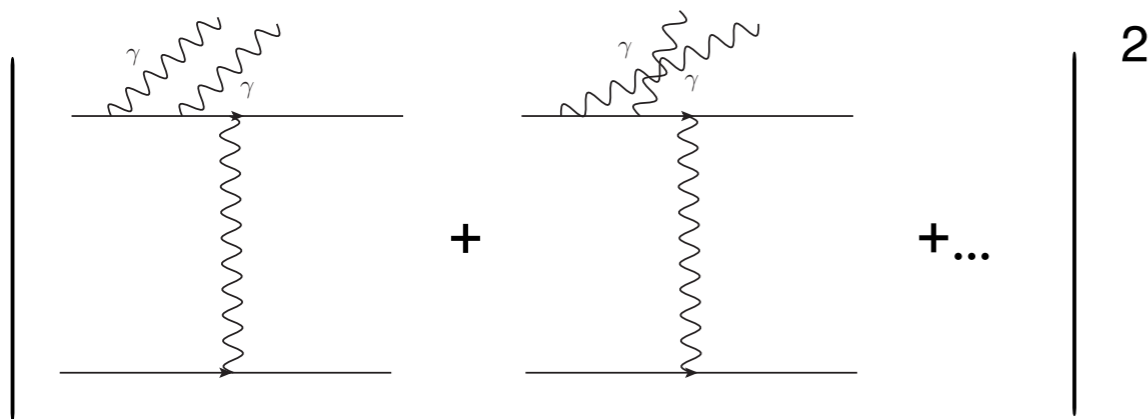
In order to remove IR divergent terms in quadratic cross section it is required to consider:

1. Photon emission from one-loop diagrams
2. Two photon photon emission



$$\underline{\sigma_Q^\gamma} = \frac{1}{2} \sigma^\gamma = \frac{\pi^2}{s} \operatorname{Re} [(-\delta_1^\lambda + R_1)^* M_1^+ M_0]$$

$$R_1 = -4B \log \frac{\sqrt{s}}{2\omega} - \log^2 \frac{s}{em^2} + 1 - \frac{\pi^2}{3} + \log^2 \frac{u}{t}$$

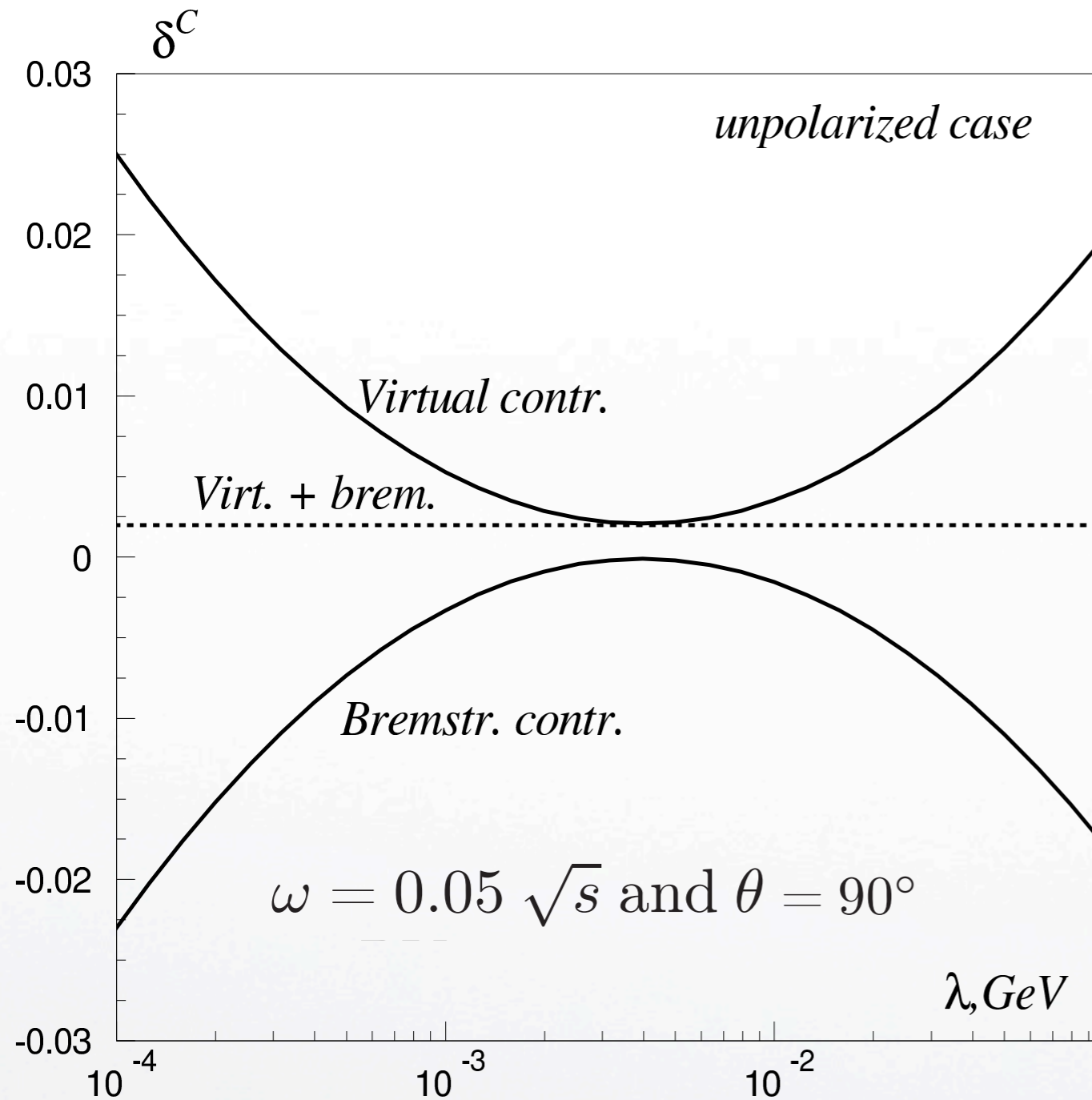


$$\underline{\sigma_Q^{\gamma\gamma}} = \frac{1}{2} \sigma^{\gamma\gamma} = \frac{1}{4} \left(\frac{\alpha}{\pi}\right)^2 \left( \left| -\delta_1^\lambda + R_1 \right|^2 - R_2 \right) \sigma_0$$

$$R_2 = \frac{8}{3} \pi^2 \left( \log \frac{tu}{m^2 s} - 1 \right)^2$$



# Quadratic correction: photon emission



$$\delta^C = (\sigma^C - \sigma^0) / \sigma^0$$

The plot for  $\theta = 90^\circ$  and  $E_{lab} = 11$  GeV, clearly demonstrates that the relative correction to unpolarized cross section is independent on the photon mass  $\lambda$ .

We can also see the quadratic dependence in log scale of  $\lambda$  for the both virtual and bremsstrahlung contributions.

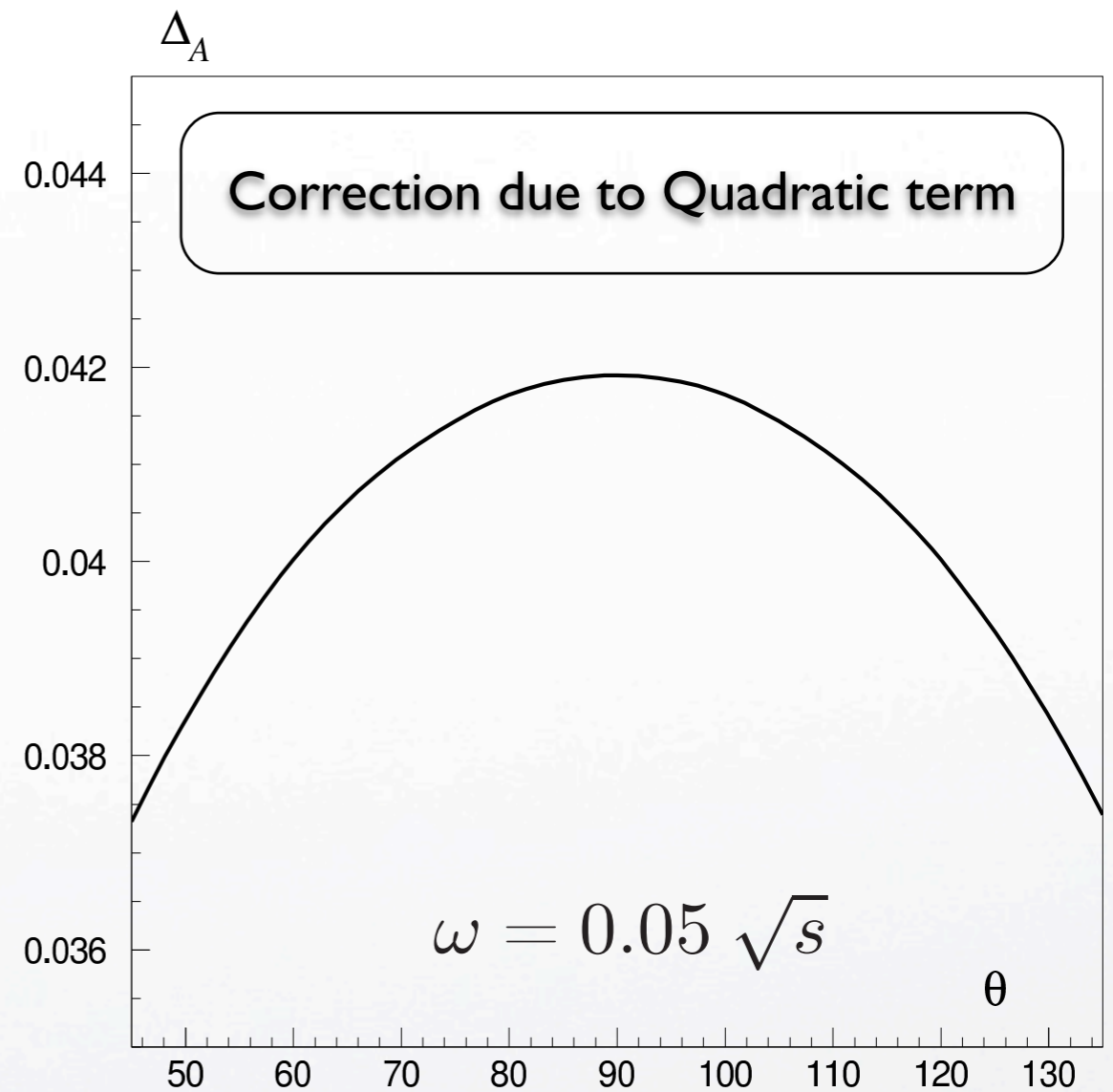
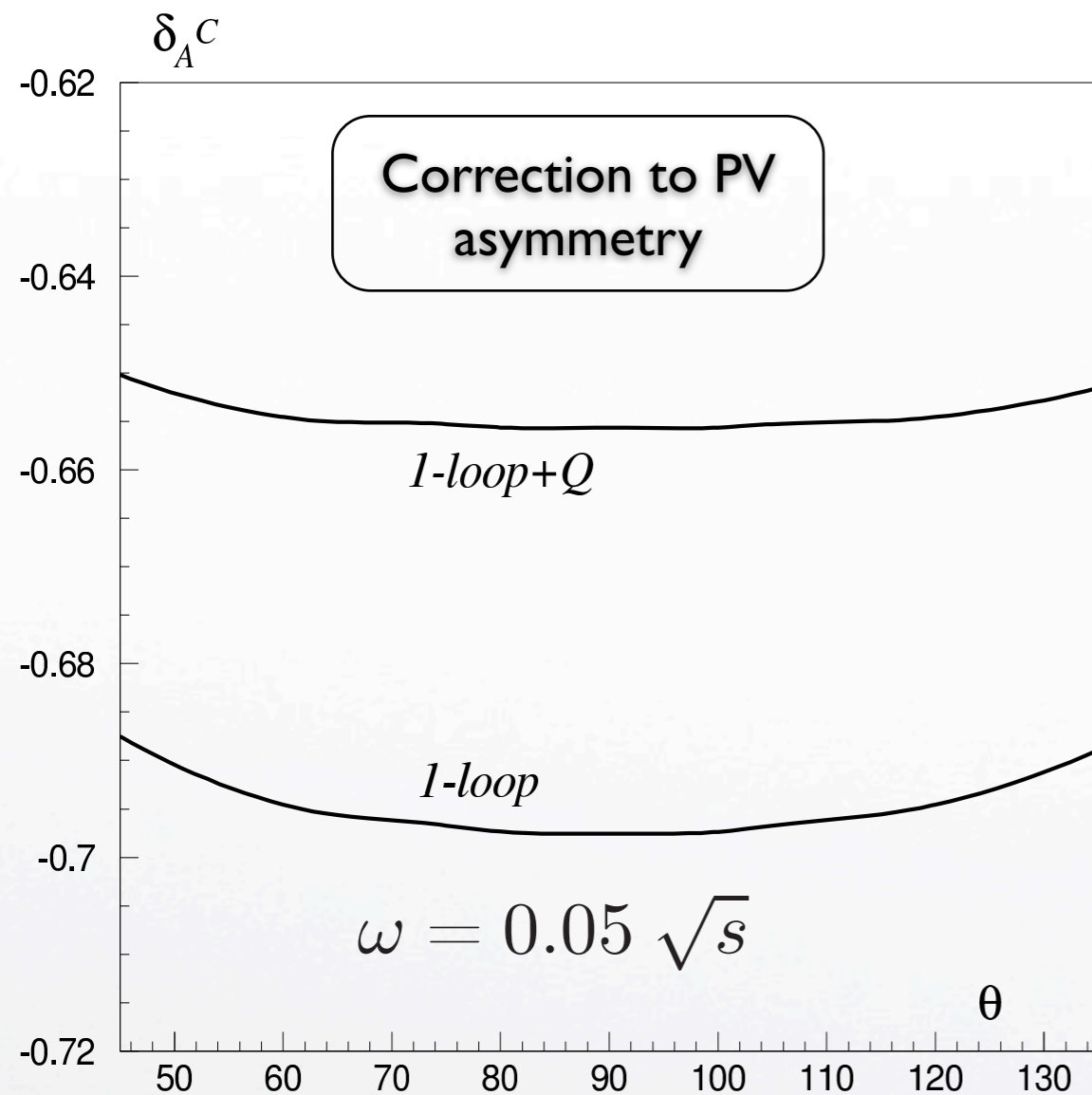


# Quadratic correction: results



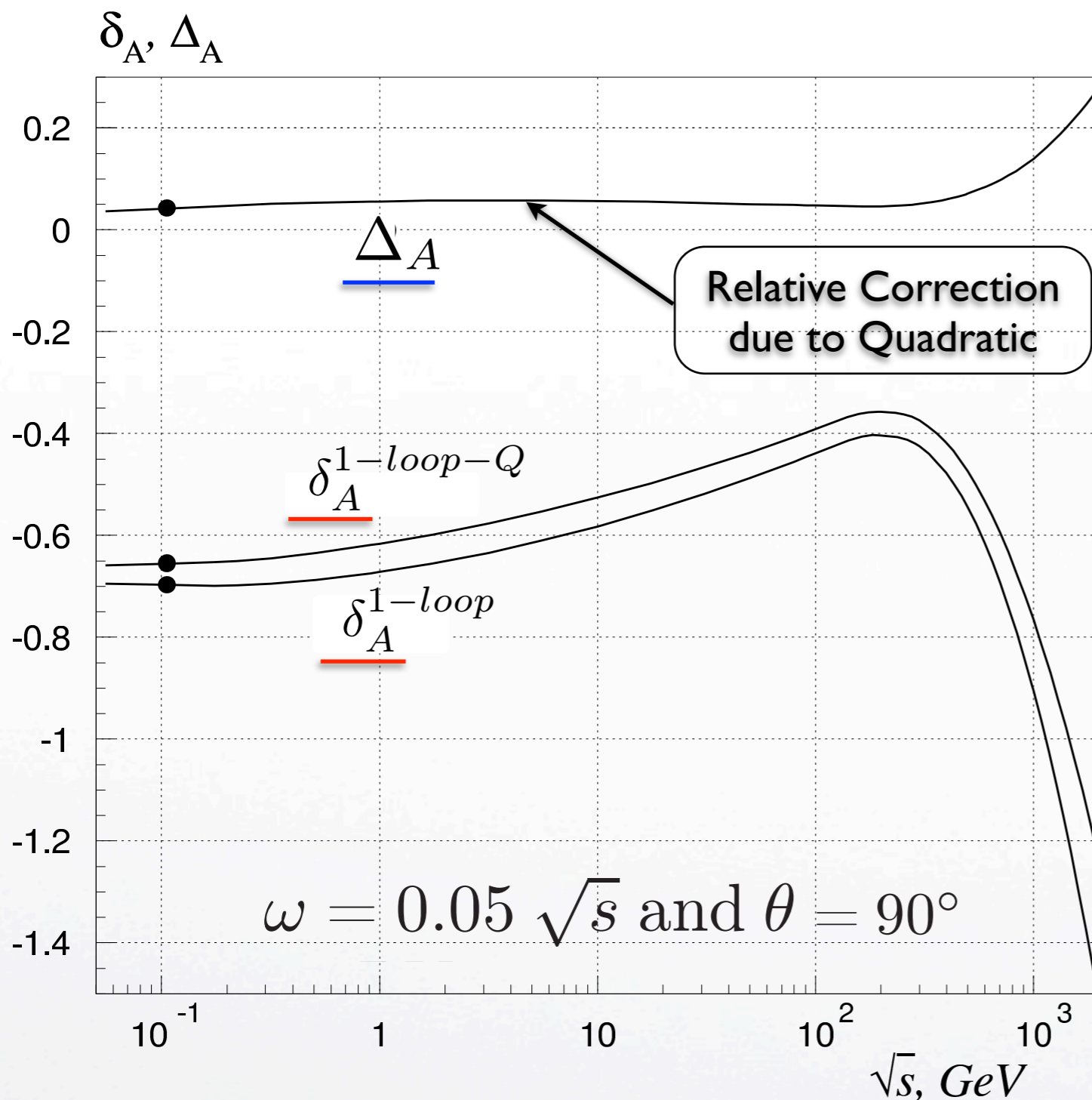
$$\delta_A^C = (A_{LR}^C - A_{LR}^0) / A_{LR}^0.$$

$$\Delta_A = (A_{LR}^{1\text{-loop}+Q} - A_{LR}^{1\text{-loop}}) / A_{LR}^0$$



$E_{\text{lab}} = 11 \text{ GeV}$

# Quadratic correction: results



$$\underline{\delta_A^C} = (A_{LR}^C - A_{LR}^0) / A_{LR}^0$$

$$\underline{\Delta_A} = (A_{LR}^{1-loop+Q} - A_{LR}^{1-loop}) / A_{LR}^0$$

The scale of the Q-part contribution in the low-energy region is approximately constant, but starting from  $\sqrt{s} \geq m_Z$ , where the weak contribution becomes comparable with electromagnetic, the effect of Q-part grows sharply.

This effect of increasing importance of two-loop contribution at higher energies may have a significant effect on the asymmetry measured at the future  $e^- e^-$ -colliders.



# Two-Loops Contribution



# Two-Loops Contribution



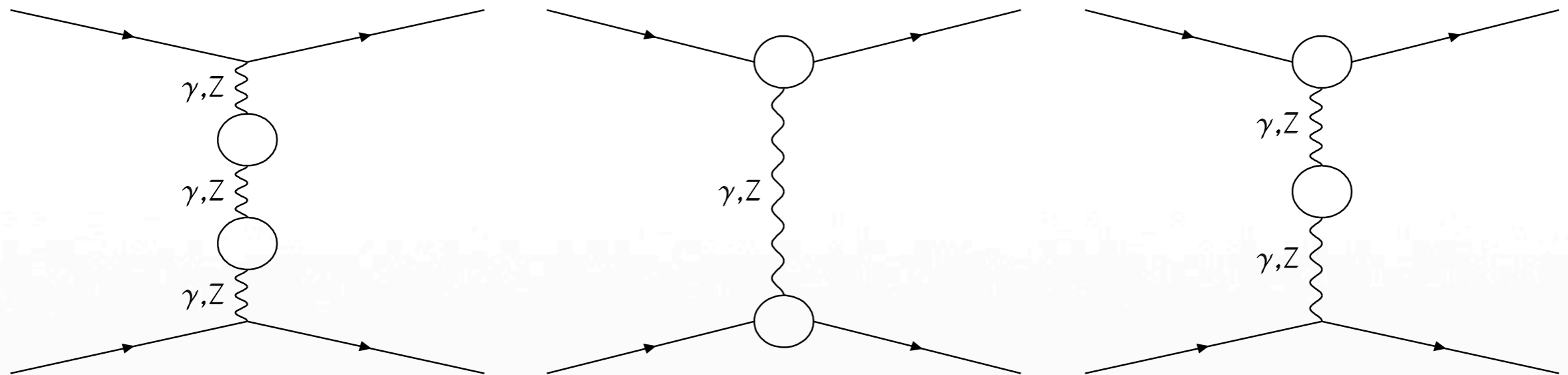
We split two-loops contribution into subsets of the gauge invariant classes:

- Separated phase space contribution (BSE + Ver)<sup>2</sup>
- Ladder, decorated boxes and boxes with electron self-energies
- Two-loops vertex correction (double vertices) and self energy diagrams

$$\sigma_T = \frac{\pi^3}{s} \operatorname{Re} M_2 M_0^+ \propto \alpha^4$$



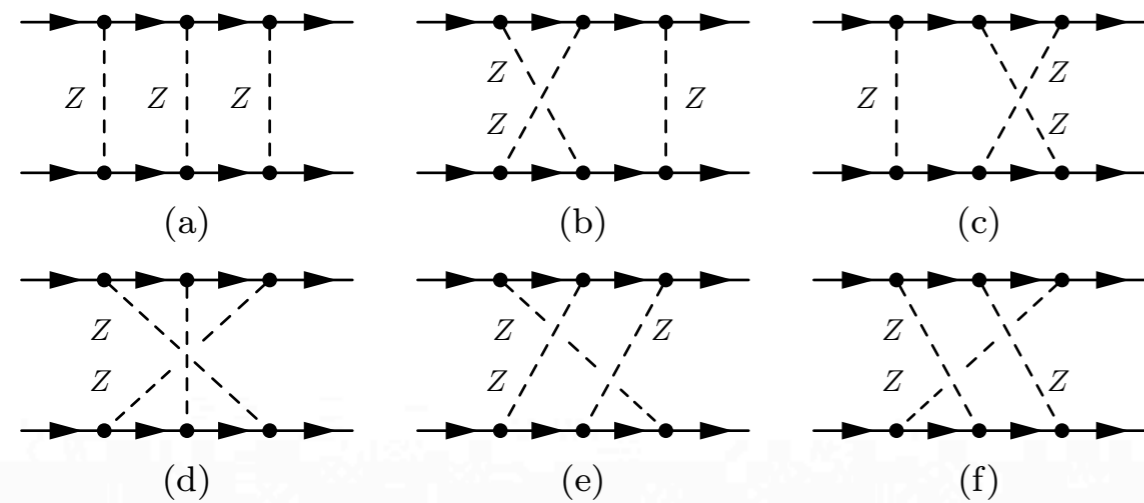
# $(\text{BSE}+\text{Ver})^2$ Two-Loops Contribution



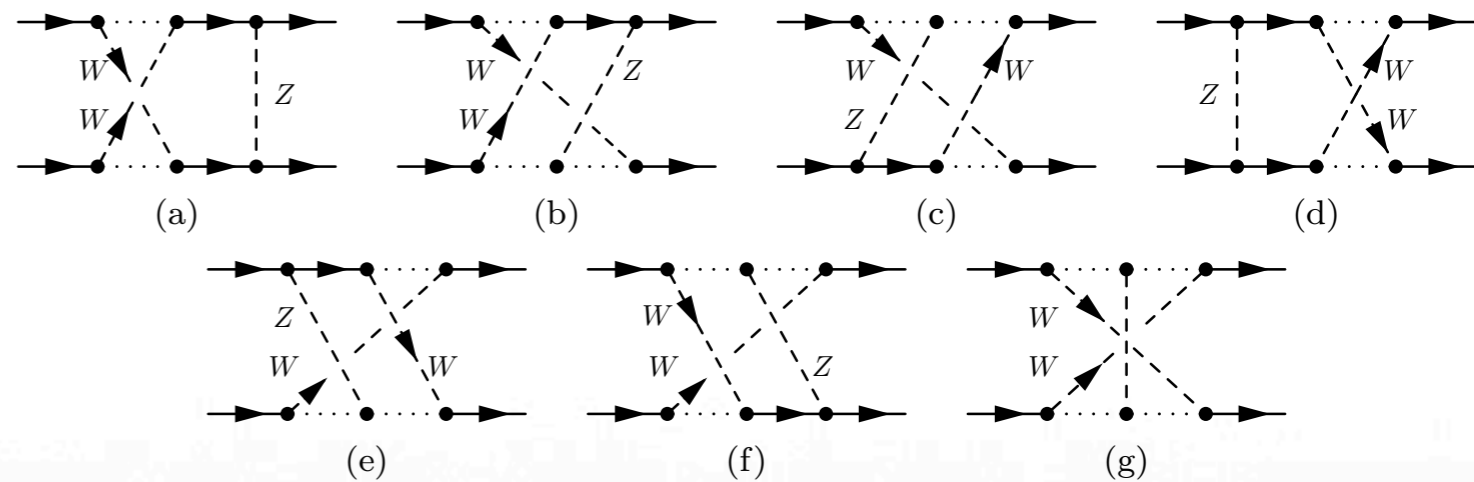
Two-loops t-channel diagrams from the gauge-invariant set of vertices and boson self-energies. Here, the circles represent the contributions of self-energies and vertex functions.



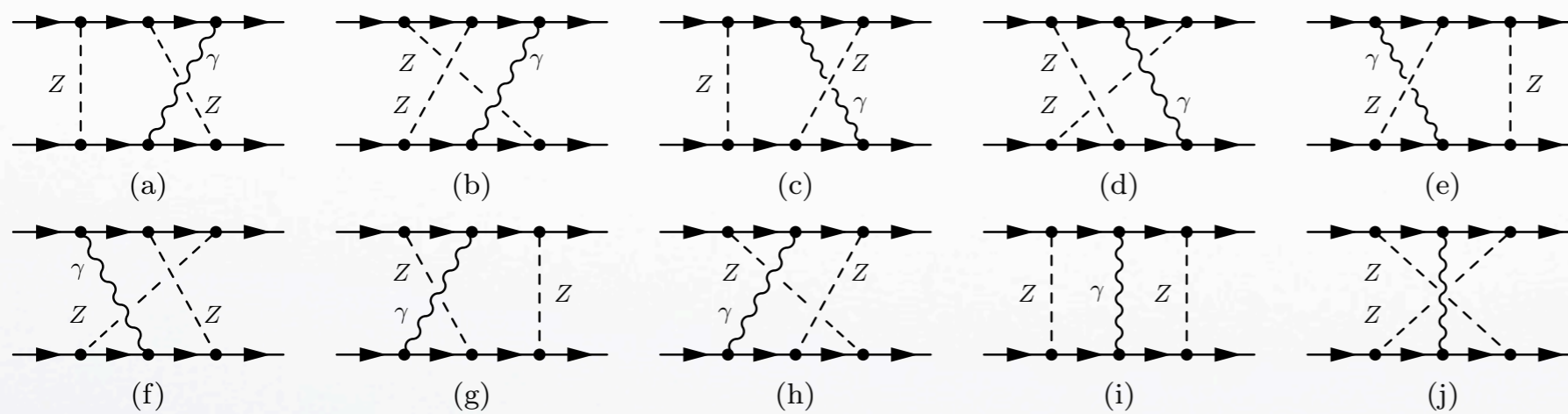
# Ladder-Box Diagrams



Diagrams with ZZZ exchange.



Diagrams with WWZ exchange.



Diagrams with ZZγ exchange.

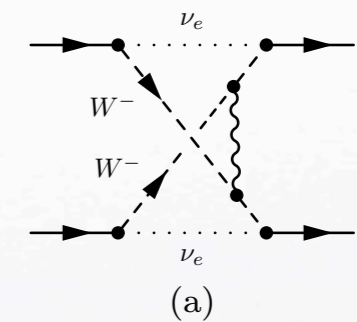
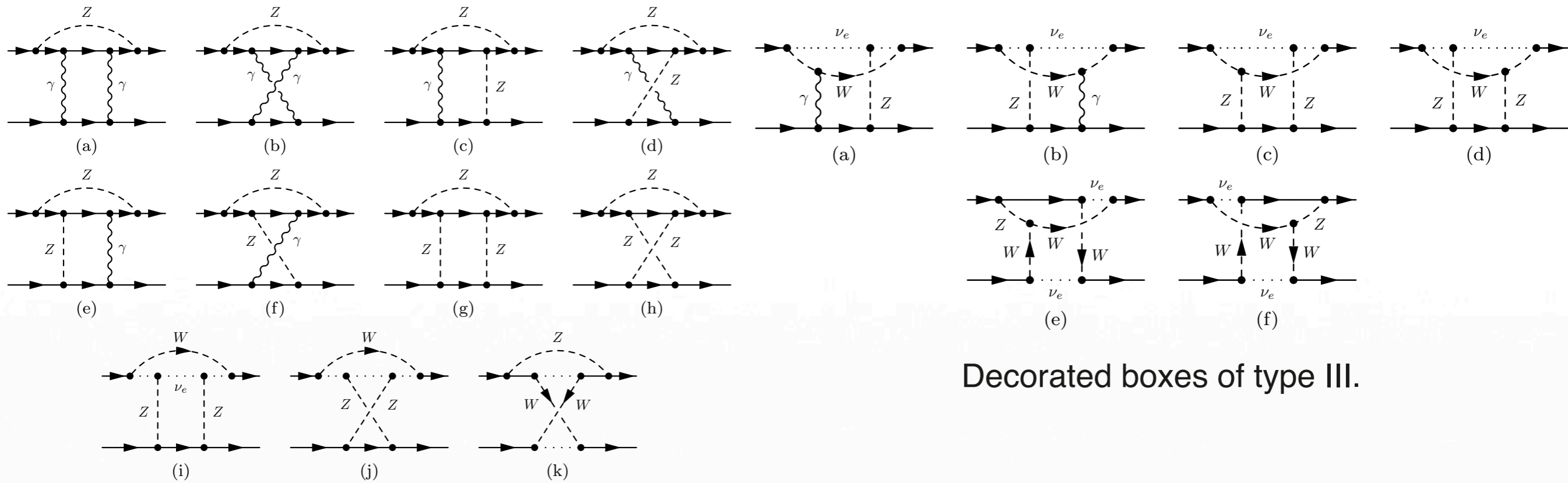


Diagram with W W γ exchange.



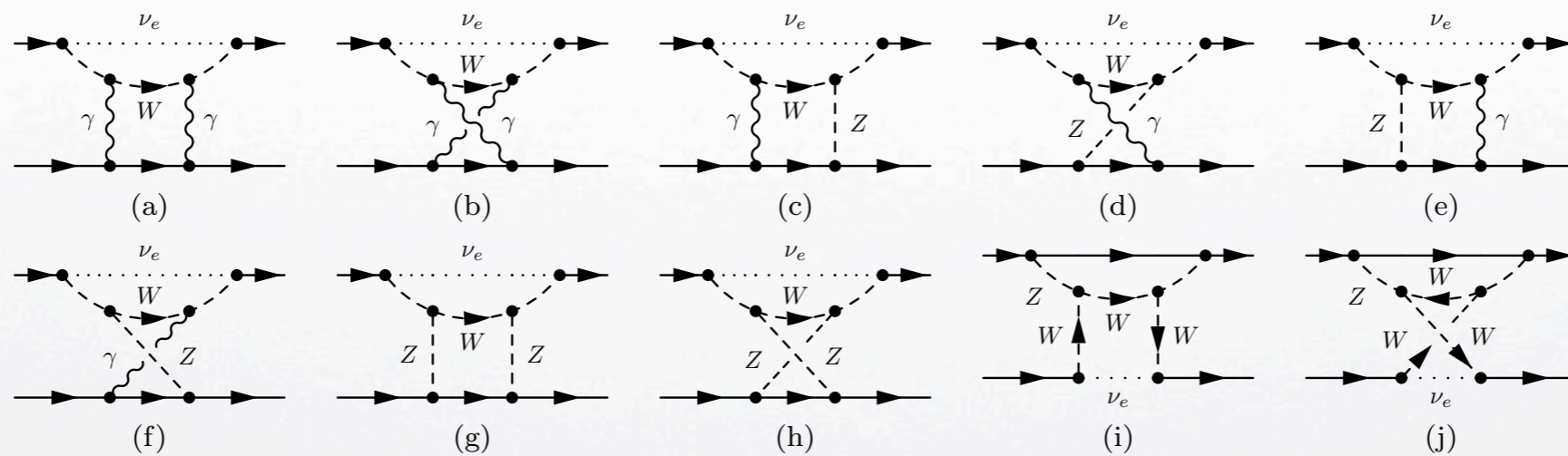


# Decorated-Box Diagrams



Decorated boxes of type III.

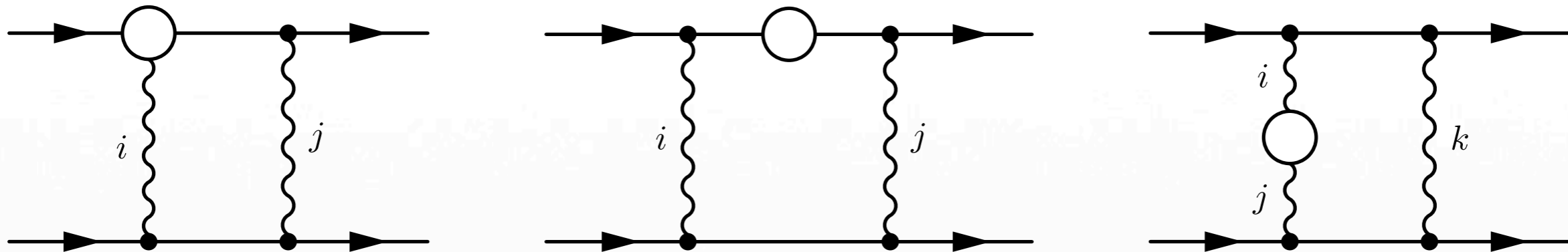
Decorated boxes of type I.



Decorated boxes of type II.



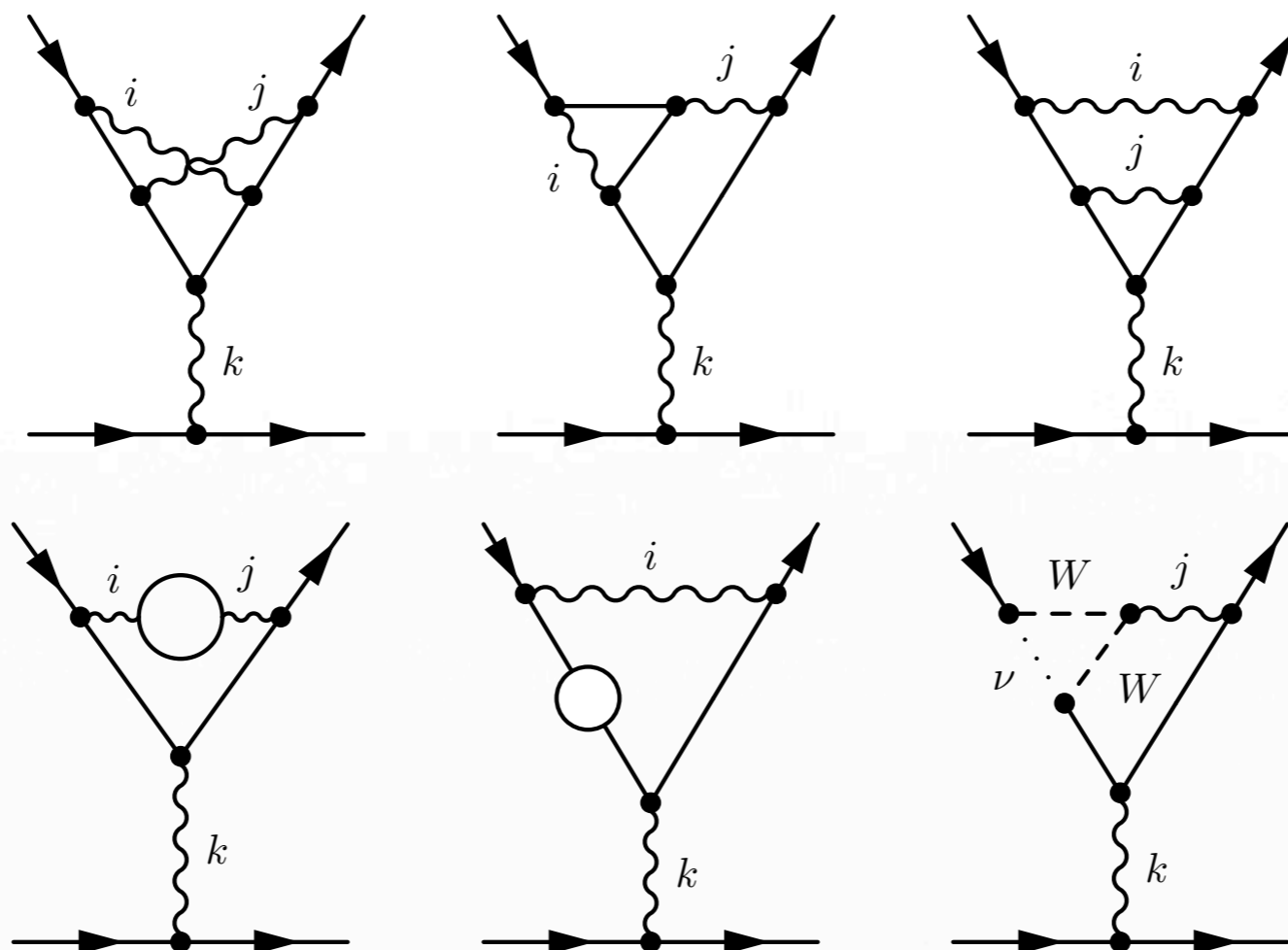
# Boxes with Lepton Self-Energy



Boxes with vertices (VB), fermion self-energy boxes FSEB and boson self-energy boxes BSEB.



# Double Vertices



Two loops electron vertices



# Final Expressions



Combining all the terms together, we get **the infrared-finite result** at one-loop level

$$\sigma_{\text{NLO}} = \sigma_1 + \sigma_1^\gamma = \frac{\alpha}{\pi} [R_1 + \delta_1^f] \sigma^0,$$

and two-loop level

$$\begin{aligned} \sigma_{\text{NNLO}} &= \sigma_Q^V + \sigma_T^V + \sigma_2^\gamma + \sigma^{\gamma\gamma} = \left(\frac{\alpha}{\pi}\right)^2 [R_1 \delta_1^f + \frac{1}{2}R_1^2 - \frac{1}{2}R_2 + \delta_Q^f + \delta_T^f] \sigma^0 = \\ &= \underline{\sigma_O^f} + \underline{\sigma_B^f} + \underline{\sigma_Q^f} + \underline{\sigma_T^f}, \end{aligned}$$

where:

$$\sigma_O^f = \frac{\alpha}{\pi} R_1 \sigma_{\text{NLO}},$$

$$\sigma_B^f = -\frac{1}{2} \left(\frac{\alpha}{\pi}\right)^2 (R_1^2 + R_2) \sigma^0,$$

$$R_1 = -4B \log \frac{\sqrt{s}}{2\omega} - \left(\log \frac{s}{m^2} - 1\right)^2 + 1 - \frac{\pi^2}{3} + \log^2 \frac{u}{t}, \quad R_2 = \frac{8}{3} \pi^2 B^2, \quad B = \log \frac{tu}{m^2 s} - 1.$$



# NNLO Numerical Results



For the orthogonal kinematics:  $\theta = 90^\circ$

Type of contribution	$\delta^C$	$\delta_A^C$	Published
NLO	-0.1145	-0.6953	PRD'10, YaF'12
...+(O+B)/2+Q	-0.1125	-0.6536	PRD'12
...+(O+B)/2+ BBSE+VVer+ VerBSE	-0.1201	-0.6420	YaF'13
...+ double boxes	-0.1201	-0.6534	EPJ'12
...+NNLO QED	-0.1152	-0.6500	
...+SE and Ver in boxes	-0.1152	-0.6503	
...+NNLO EW Ver		under way	

$$\delta_A^C = \frac{A_{LR}^C - A_{LR}^0}{A_{LR}^0}$$

$$\delta^C = \frac{\sigma_{00}^C - \sigma_{00}^0}{\sigma_{00}^0}$$

$$\omega = 0.05\sqrt{s}$$

“...” means all contributions from the lines above



# New Physics(NP)



# Subtractive Scheme



We use subtractive renormalization scheme which is more suitable for the analysis of new physics. We can choose scales of subtractive scheme so it will exactly reproduce the on-shell renormalization scheme results.

As an example we can use the following structure of the UV divergent part of the amplitude up to one-loop:

$$M^{UV}(q) = (a_1 + a_2 q^2) \Delta \quad \text{where} \quad \Delta = \frac{2}{4 - D}$$

And in order to satisfy HRC renormalization conditions, we have:

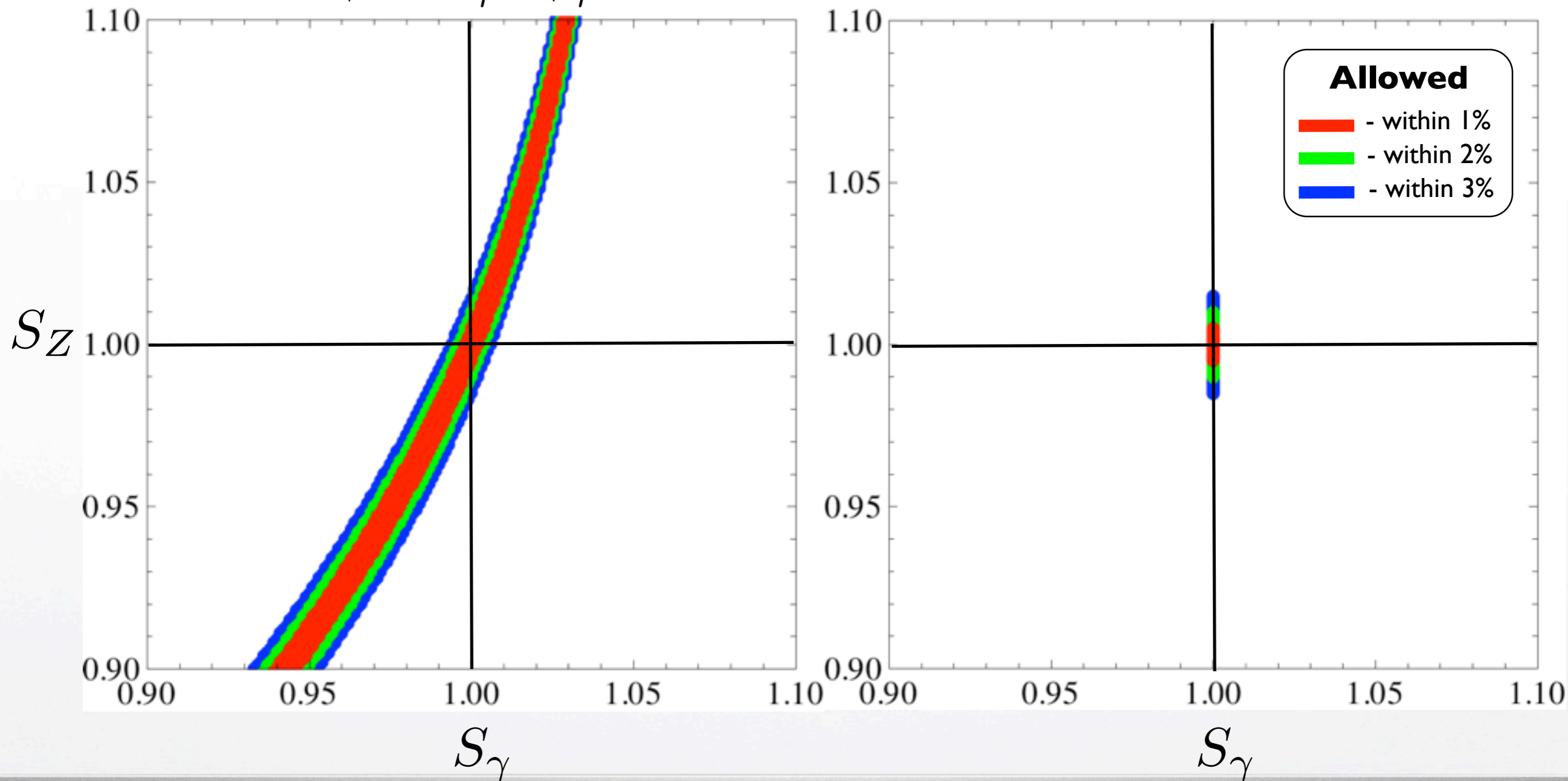
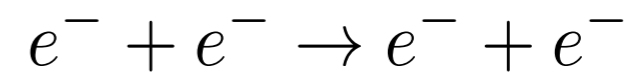
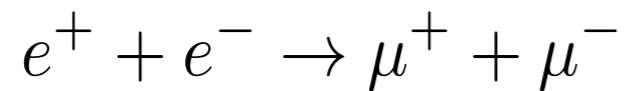
$$\hat{\Sigma}_{V_1 V_2}(q^2) = \Sigma_{V_1 V_2}(q^2) - \epsilon \text{Re} \Sigma_{V_1 V_2}(m_{V_1}^2) - \text{Re} \partial_{q^2} \Sigma(q^2) \Big|_{q^2 = \Lambda_{V_1 V_2}^2} (q^2 - m_{V_1}^2)$$

here  $\epsilon = 0$  for  $V_1 V_2 = \gamma\gamma$  and  $\epsilon = 1$  for all other cases of  $V_1 V_2$ .

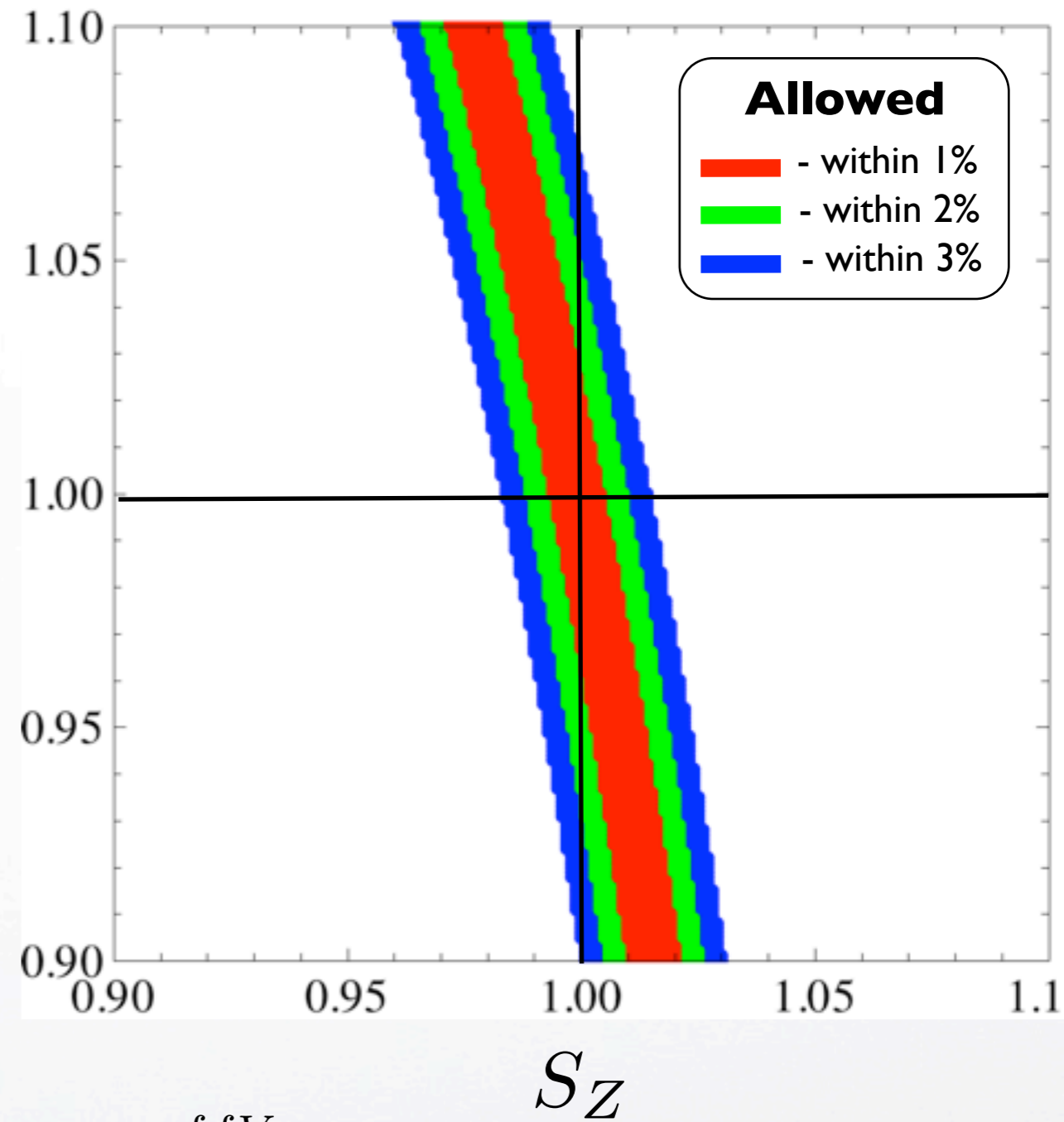
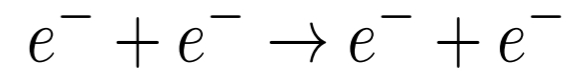
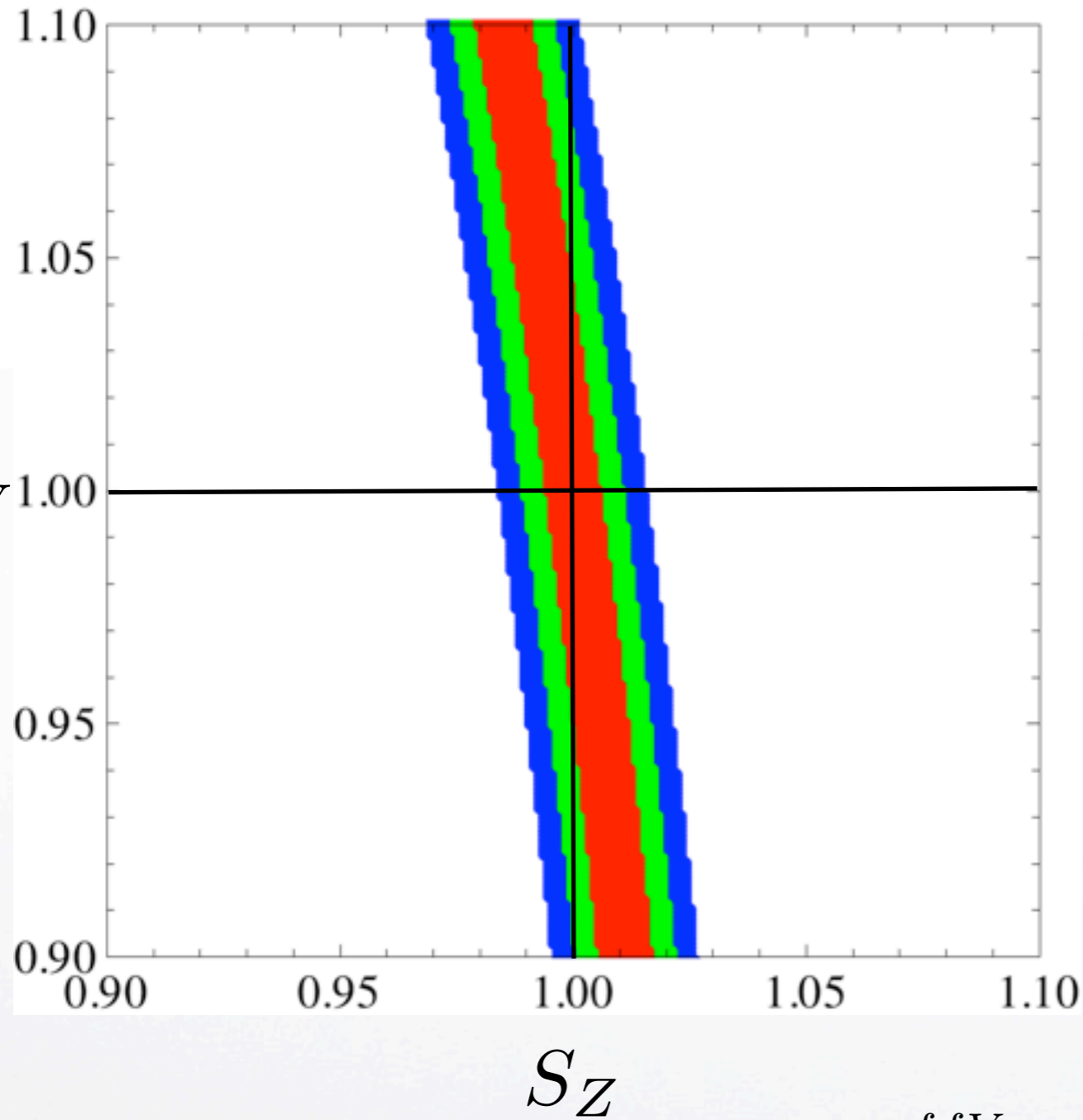
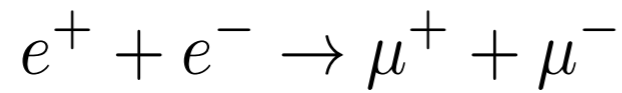
$$\hat{\Gamma}_{\mu}^{ffV}(q^2) = \Gamma_{\mu}^{ffV}(q^2) - \Gamma_{\mu}^{ffV}(0)$$

Scale	Value (GeV)
$\Lambda_{\gamma\gamma}$	0.0
$\Lambda_{\gamma Z}$	12.2945
$\Lambda_{ZZ}$	3.1543
$\Lambda_{WW}$	3.7142

- The same as in the Standard Model, but with couplings scaled:  $\Gamma_{\mu}^{ffV} \rightarrow S_V \cdot \Gamma_{\mu}^{ffV}$







$$\Gamma_{\mu}^{ffV} \rightarrow S_V \cdot \Gamma_{\mu}^{ffV}$$



# New Vector Boson



- We will consider two cases of the NP particle:
  - Massive vector boson with parity conserving (PC) coupling.
  - Massive vector boson with parity violating (PV) coupling.

For the PC vector boson we have:

$$\Gamma_{\mu}^{ff\gamma'} = \underline{S_{\gamma'}} \cdot ie\gamma_{\mu}$$

$$\Pi_{\mu\nu} = \frac{ig_{\mu\nu}}{q^2 - \underline{m_{\gamma'}^2} + i\epsilon}$$

For the PV vector boson we have:

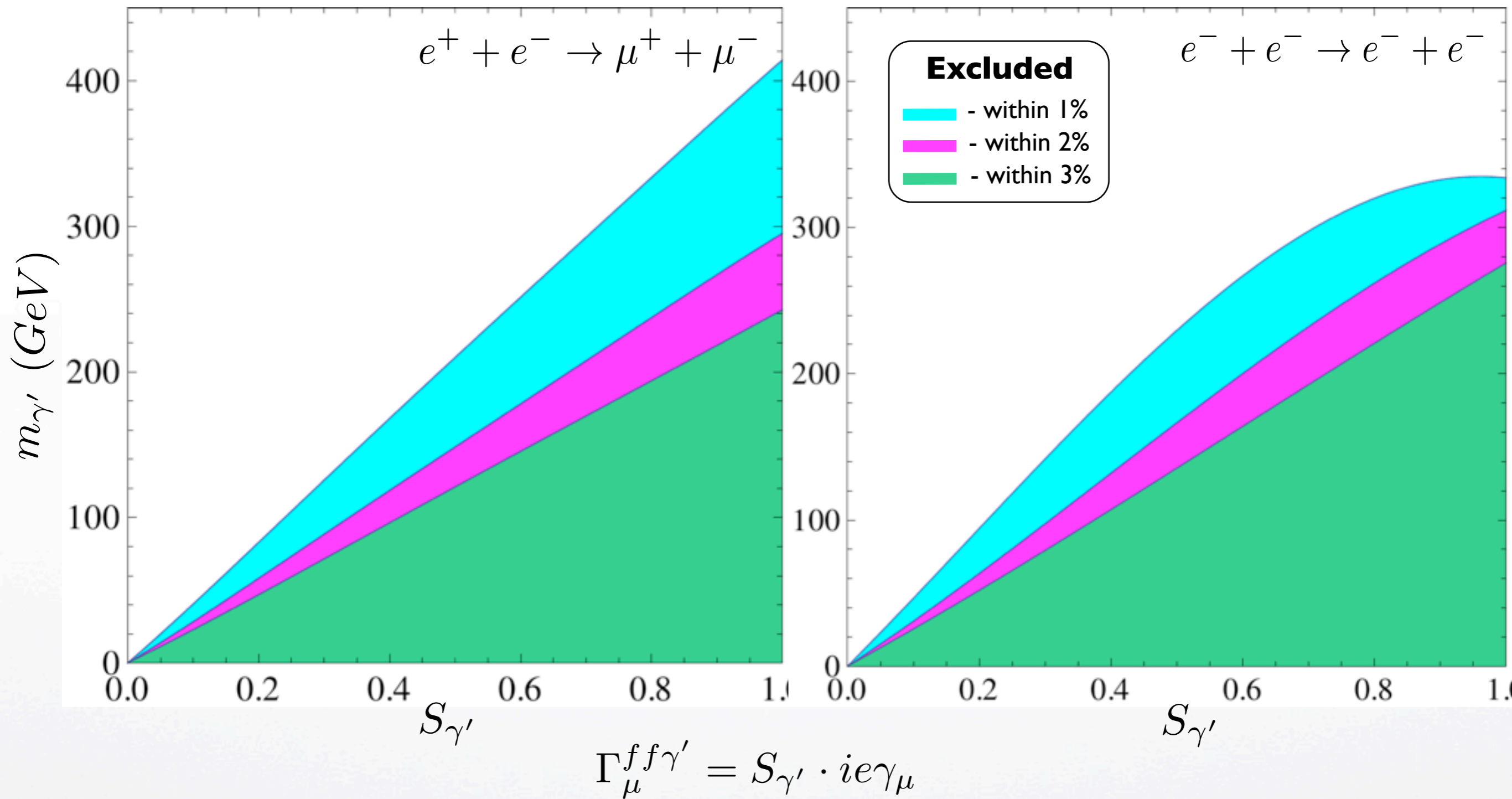
$$\Gamma_{\mu}^{ffZ'} = ie(\underline{S_R^{Z'}} \gamma_{\mu}\omega_{+} + \underline{S_L^{Z'}} \gamma_{\mu}\omega_{-})$$

$$\Pi_{\mu\nu} = \frac{ig_{\mu\nu}}{q^2 - \underline{m_{Z'}^2} + i\epsilon}$$

$$\omega_{\pm} = \frac{1 \pm \gamma_5}{2}$$



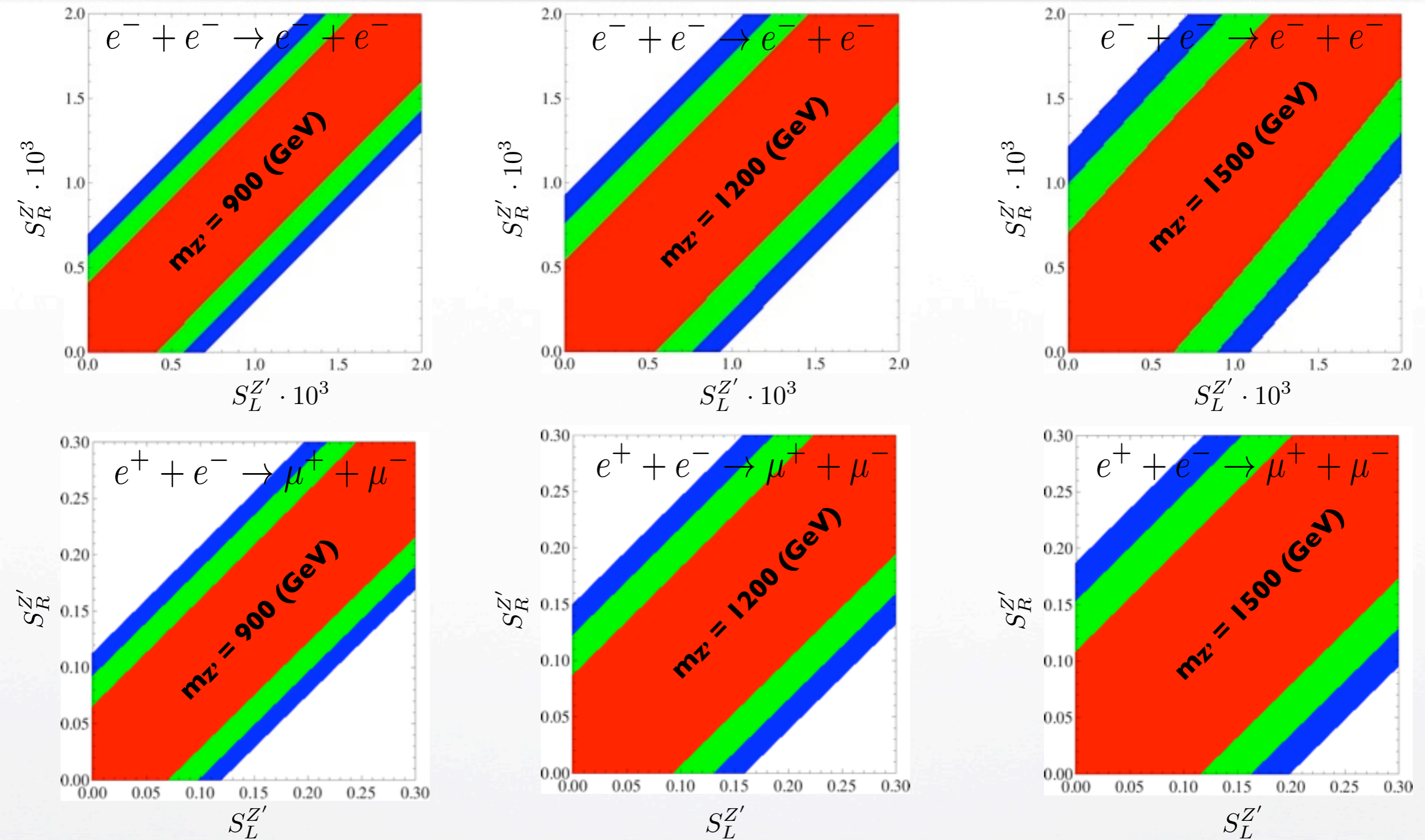
# New Vector Boson: Parity-Conserved



Including additional massive boson requires calculation of 820 graphs at one-loop level.



# New Vector Boson: Parity-Violating



$$\Gamma_{\mu}^{ffZ'} = ie(S_R^{Z'} \gamma_{\mu} \omega_+ + S_L^{Z'} \gamma_{\mu} \omega_-)$$



# Conclusion

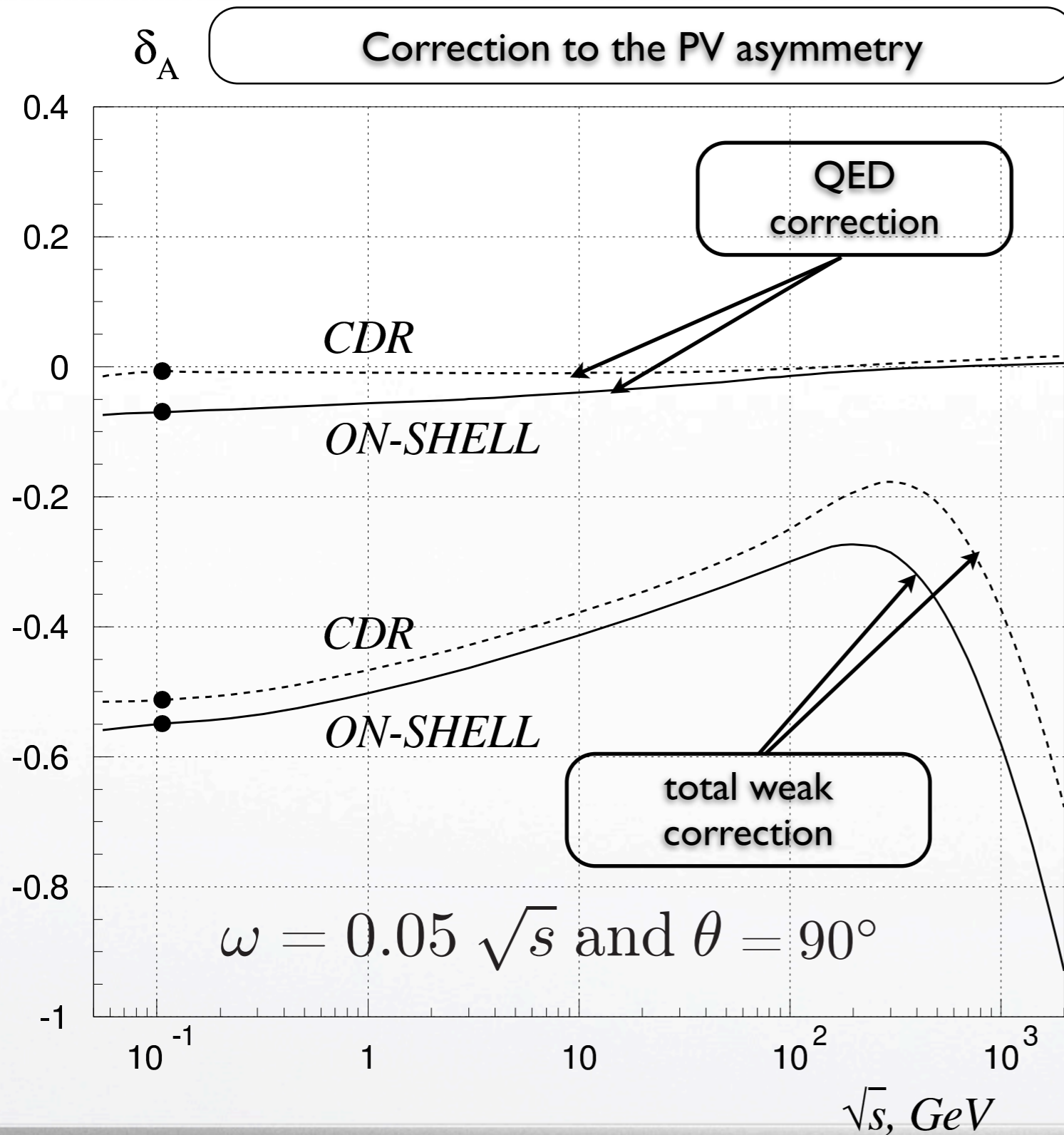


- EWC corrections depend quite significantly on the energy and scattering angles.
- At the MOLLER kinematic conditions, the quadratic (Q-part) EWC we considered here can increase the asymmetry up to  $\sim 4\%$ .
- For the high-energy region  $\sqrt{s} \sim 2000$  GeV the contribution of the quadratic EWC we estimated can reach  $+30\%$ .
- Excellent agreement obtained between the results calculated "by hand" and semi-automatically serves as a good illustration of opportunities offered by FeynArts, FormCalc, LoopTools, and FORM.
- So far, dominant two-loops contributions to the PV asymmetry are at the order of  $1\%$  and they are coming from  $(Ver + BSE)^2$  and double boxes. Their values have opposite sign and hence completely cancel each other, leaving Q-part as a biggest contributor to the asymmetry at the order of  $\alpha^4$ .
- MOLLER will have significant sensitivity to the detection of parity-violating vector boson.



# Backup Slides

# One-loop in different schemes: asymmetry



$$\delta_A^C = \frac{A_{LR}^C - A_{LR}^0}{A_{LR}^0}$$

- Correction to asymmetry differ in two schemes at the order of 10%.

- Higher order contributions are important!